Check for updates

BOREAS An international journal of Quaternary research

The impact of the structural framework of the North German Basin on Pleistocene tunnel-valley formation

JÖRG LANG, ANKE BEBIOLKA, VERA NOACK, JULIA SCHÜTZKE, SARAH WEIHMANN AND SONJA BREUER

BOREAS

Lang, J., Bebiolka, A., Noack, V., Schützke, J., Weihmann, S. & Breuer, S.: The impact of the structural framework of the North German Basin on Pleistocene tunnel-valley formation. *Boreas*. https://doi.org/10.1111/bor.12694. ISSN 0300-9483.

Tunnel valleys are impressive subglacial erosional landforms and may attain depths of almost 600 m. Climatic and glaciological factors exert the primary control on tunnel-valley formation. Furthermore, regional geological features, e.g. faults and salt structures, have been suggested as controlling factors for tunnel-valley formation. To improve the understanding of the impact of these geological factors on tunnel-valley incision, we compare the distribution and orientations of buried Pleistocene tunnel valleys in the North German Basin with regional geological features, such as basin geometry and infill, faults and salt structures. Our analysis shows that deep tunnel valleys are restricted to areas with thick erodible Cenozoic deposits. The correlation between the trends of tunnel valleys, faults and salt structures varies between the analysed regions. The orientations of tunnel valleys commonly follow the trends of faults and salt structures in regions where the structural trend is NNW–SSE to east–west and ice-flow directions were approximately parallel to this trend. However, correlations are rarely observed if the regional structural trend is NW–SE to WNW–ESE and ice advances occurred thus normal or oblique to the regional fault trend. Potential future tunnel-valley incision is regarded as a major challenge for the long-term safety of radioactive waste repositories because incision may reach depths under consideration for repositories. The presence and orientations of faults and salt structures, however, do not provide consistent indicators for future tunnel-valley incision.

Jörg Lang (joerg.lang@bgr.de), Anke Bebiolka, Vera Noack and Sonja Breuer, Bundesanstalt für Geowissenschaften und Rohstoffe (BGR), Stilleweg 2, 30655 Hannover, Germany; Julia Schützke and Sarah Weihmann, Lehrstuhl für Endlagersicherheit (ELS), RWTH Aachen, Wüllnerstraße 2, 52062 Aachen, Germany; *received 4th October 2024, accepted 21st December 2024.*

Tunnel valleys are common features in formerly glaciated sedimentary basins that may attain depths of almost 600 m, for example in the North German Basin (Fig. 1). Characteristic features of tunnel valleys include undulating longitudinal basal profiles, steep flanks and abrupt terminations, which indicate incision by the channelized drainage of pressurized meltwater beneath ice sheets (Huuse & Lykke-Andersen 2000; Kehew *et al.* 2012; Van der Vegt *et al.* 2012; Kirkham *et al.* 2021, 2024a, b; Breuer *et al.* 2023b; Gegg & Preusser 2023). The formation and characteristics of tunnel valleys are primarily controlled by climatic and glaciological factors (Kehew *et al.* 2012; Sandersen & Jørgensen 2012, 2022; Bjarnadóttir *et al.* 2017; Kirkham *et al.* 2024a, b). The geology of the substratum, particularly the erodibility and hydraulic conductivity (Ó Cofaigh 1996; Huuse & Lykke-Andersen 2000; Boulton *et al.* 2009; Kehew *et al.* 2012), is considered another important control on subglacial erosion, meltwater-drainage pattern and tunnel-valley formation. In general, tunnel-valley formation is restricted to areas comprising erodible (commonly sedimentary and poorly lithified) rocks. In areas characterized by resistant (commonly crystalline) bedrock, incision by basal meltwater occurs rather upwards into the ice than into the substratum and meltwater is drained through R-type channels (Piotrowski 1994; Boulton *et al.* 2009; Kehew *et al.* 2012). In such settings, eskers replace tunnel valleys as the predominant meltwater-related geomorphic feature (Boulton *et al.* 2009). At higher resolutions, the complexity increases and features such as basin geometry (e.g. Piotrowski 1994; Stackebrandt 2009; Breuer *et al.* 2023b; Kirkham *et al.* 2024b), lithology (e.g. Janszen *et al.* 2012; Sandersen & Jørgensen 2012; Ottesen *et al.* 2020), faults (e.g. Reicherter *et al.* 2005; Stackebrandt 2009; Wenau & Alves 2020; Brandes *et al.* 2022; Sandersen & Jørgensen 2022) and salt structures (e.g. Al Hseinat & Hübscher 2014; Lang *et al.* 2014; Wenau & Alves 2020) have been suggested as controlling factors of tunnel-valley formation.

Tunnel-valley fills are typically dominated by subglacial and proglacial meltwater deposits that indicate ice-margin retreat. If tunnel valleys remain underfilled after deglaciation, they commonly act as depocentres for post-glacial sedimentation (Ehlers & Linke 1989; Piotrowski 1994; Lang *et al.* 2012, 2015; Janszen *et al.* 2013; Gegg & Preusser 2023; Kirkham *et al.* 2024b). Therefore, the infills of tunnel valleys represent important archives of past glaciations and changing environmental conditions. Tunnel-valley fills are economically important as they may for example contain reservoirs for groundwater or hydrocarbons (BurVal Working Group 2006; Huuse *et al.* 2012). Furthermore, tunnel-valley incision beneath potential future ice sheets is regarded as a major

DOI 10.1111/bor.12694
© 2025 The Author(s). *Boreas* published by John Wiley & Sons Ltd on behalf of The Boreas Collegium. This is an open access article under the terms of the Creative Commons Attribution License, which permits use, distribution and reproduction in any medium, provided the original work is properly cited.

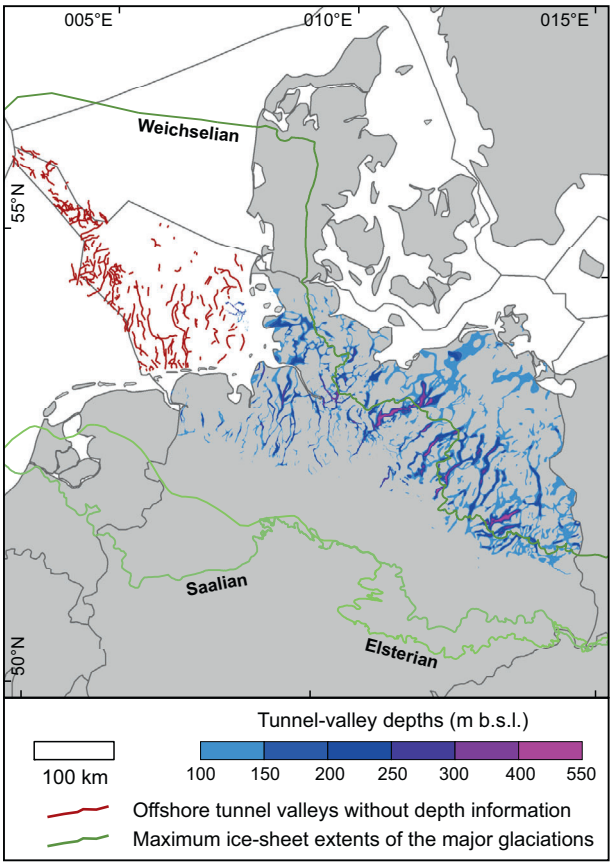

Fig. 1. Buried tunnel valleys in northern Germany (Breuer *et al.* 2023b; Jagemann & Müller 2023) and the German North Sea sector (Lutz *et al.* 2009; Hepp *et al.* 2012; Lohrberg *et al.* 2022b). Further tunnel valleys exist closer to the Middle Pleistocene maximum ice-sheet extents but are generally shallower than 100 m b.s.l. The ice-sheet extents are based on Ehlers *et al.* (2011) and Winsemann *et al.* (2011).

challenge for the long-term safety of radioactive waste repositories, as incision may reach depths under consideration for the construction of such repositories (Talbot 1999; Fischer *et al.* 2021; Breuer *et al.* 2023b).

The objective of this study is to improve the understanding of the impact of regional geology on the formation, distribution and orientation of tunnel valleys in northern Germany and the German North Sea sector (Fig. 1). The major motivation behind this study is the safe disposal of radioactive waste in deep geological repositories. Understanding the geological control on tunnel-valley formation is an important contribution to long-term safety assessments, which are required to account for potential future glaciations. An extensive regional dataset on tunnel valleys, faults, salt structures and the basin fill was analysed for this study. Based on previous studies, three main hypotheses can be formulated on the impact of the structural framework of the subsurface on tunnel-valley formation: (i) tunnel valleys are preferentially incised into those parts of sedimentary basins that contain thick successions of poorly consolidated and thus erodible deposits (e.g. Stackebrandt 2004, 2009; Kehew *et al.* 2012; Ottesen *et al.* 2020; Breuer *et al.* 2023b); (ii) faults promote tunnel-valley incision and tunnel valleys align with faults, especially if these faults have been neotectonically active (e.g. Reicherter *et al.* 2005; Stackebrandt 2009; Brandes *et al.* 2022; Sandersen & Jørgensen 2022); and (iii) the presence of salt structures facilitates tunnel-valley incision (e.g. Al Hseinat & Hübscher 2014; Lang *et al.* 2014; Wenau & Alves 2020). To test these hypotheses, this study aims to identify correlations between tunnel valleys and underlying geological features.

Regional setting

The study area is located in the North German Basin, which forms part of the Southern Permian Basin in the Central European Basin System (Fig. 2). Since the latest Carboniferous, the North German Basin has experienced a complex evolution, which is reflected in its structural framework. During the Pleistocene, large parts of the North German Basin were repeatedly overridden by the Fennoscandian ice sheets (Fig. 1).

Basin evolution

The formation of the Central European Basin System was initiated during the latest Carboniferous and Early Permian by wrench tectonics between the Sorgenfrei–Tornquist Zone and the Teisseyre–Tornquist Zone to the north and the Elbe Fault System to the south (Fig. 2; Scheck *et al.* 2002; Scheck-Wenderoth & Lamarche 2005; Pharaoh *et al.* 2010). During the Late Permian to Middle Triassic, west–east-directed extension led to the formation of and strong subsidence in the NNW–SSE-striking Central Graben and the NE–SW-striking Horn Graben, Glückstadt Graben and Rheinsberg Trough (Fig. 2; Maystrenko *et al.* 2008, 2013; Pharaoh *et al.* 2010). In the Late Jurassic to Late Cretaceous, NE–SW-directed extension triggered the differentiation of NW–SE-trending sub-basins such as the Lower Saxony Basin, the Subhercynian Basin, the Grimmen Basin, the Prignitz Basin, the Brandenburg Basin and the Lusatian Basin (Fig. 2; Pharaoh *et al.* 2010).

During the Late Cretaceous to Early Palaeogene, NE–SW- and NNE–SSW-directed compression led to basin inversion (Ziegler 1990; Kley & Voigt 2008). Inversion focused along the southwestern and northeastern basin margins and triggered the reactivation of normal faults as reverse faults and the uplift of basement blocks (Lohr *et al.* 2007; Kley & Voigt 2008; Pharaoh *et al.* 2010; Voigt *et al.* 2021). Areas that were especially strongly affected by the inversion include the Lower Saxony Basin, Subhercynian Basin, Lusatian Basin, Prignitz Basin and Grimmen Basin (Fig. 2; Pharaoh *et al.* 2010).

The Cenozoic evolution of the North German Basin was characterized by west–east-directed extension and

15023085, 0, Downloaded from https://onlinelibrary.wiley.com/doi/10.1111/bor.12694 by Rwth Aachen University Universitatsbibliothek- 021000, Wiley Online Library on [27/01/2025]. See the Terms and Conditions (https://onlinelibrary.wiley.com/terms-and-conditions) on Wiley Online Library for rules of use; OA articles are governed by the applicable Creative Commons License

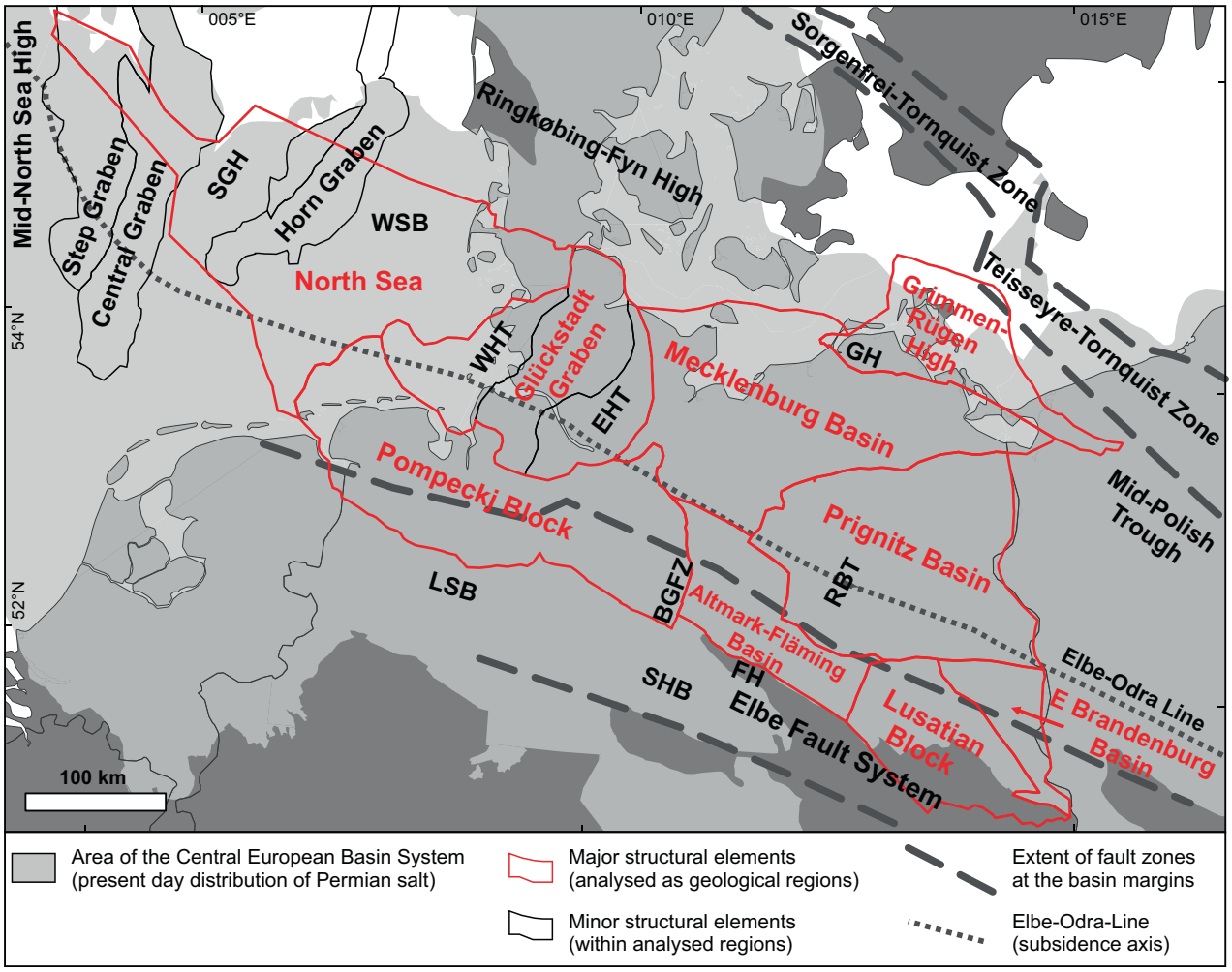

Fig. 2. Overview map of the Southern Permian Basin with major structural elements. The light grey area is the extent of the Central European Basin System, indicated by the presence of Permian evaporites (Doornenbal & Stevenson 2010). Geological regions used in the data analysis are indicated in red. Further structural elements are labelled in black (BGFZ = Braunschweig-Gifhorn Fault Zone; EHT = East Holstein Trough; FH = Flechtingen High; GH = Grimmen High; LSB = Lower Saxony Basin; RBT = Rheinsberg Trough; SGH = Schillgrund High; SHB = Subhercynian Basin; WHT = West Holstein Trough; WSB = West Schleswig Block) (compiled from Doornenbal & Stevenson 2010; Warsitzka *et al.* 2019). The extents of the Sorgenfrei–Tornquist Zone and the Teisseyre–Tornquist Zone and the Elbe Fault System at the northern and southern basin margins, respectively, are indicated (Scheck *et al.* 2002; Scheck-Wenderoth & Lamarche 2005).

subsidence, especially in the North Sea and the Glückstadt Graben (Scheck-Wenderoth & Lamarche 2005; Lohr *et al.* 2007; Pharaoh *et al.* 2010; Ahlrichs *et al.* 2021). Ahlrichs *et al.* (2021) suggested that the extension can be regarded as a northern continuation of the European Cenozoic rift system (cf. Ziegler 1992). The Cenozoic subsidence axis follows the NW–SE-trending Elbe-Odra Line, which is an old deep crustal boundary (Fig. 2; Ludwig 2001; Scheck *et al.* 2002).

Data on the present-day stress field in Germany are generally sparse and unevenly distributed. Stress analysis suggests a fan-like pattern of the maximum horizontal stress (S_{Hmax}) directions in the North German Basin, ranging from NW–SE in the western part of the basin to NE–SW in the eastern part of the basin (Marotta *et al.* 2002; Heidbach *et al.* 2018; Morawietz *et al.* 2020; Ahlers *et al.* 2022; Röckel *et al.* 2022). The state of horizontal compression (Bayer *et al.* 1999) suggests a preference for strike-slip and thrust-fault regimes. With increasing depth, normal faulting regimes become predominant (Ahlers *et al.* 2022; Röckel *et al.* 2022). The present-day stress field has been established since the Oligocene (Kaiser *et al.* 2005; Reicherter *et al.* 2005). Today, the North German Basin forms part of a low-strain area with horizontal shortening rates between the Alps and southern Scandinavia of less than 0.5 mm a^{-1} (Piña-Valdés *et al.* 2022). Pleistocene and Holocene faulting and historic seismicity are commonly interpreted as related to stress changes owing to glacial isostatic adjustment (Brandes *et al.* 2015, 2019).

The presence of thick Permian salt rocks had a major impact on the structural and depositional architecture of

15023885, 0, Downloaded from https://onlinelibrary.wiley.com/doi/10.1111/bor.12694 by Rwth Aachen University Universitatsbibliothek- 021000, Wiley Online Library on [27/01/2025]. See the Terms and Conditions (https://onlinelibrary.wiley.com/terms-and-conditions) on Wiley Online Library for rules of use; OA articles are governed by the applicable Creative Commons License

the basin fill. Salt rocks are mechanically weak and allow for a decoupling between supra- and sub-salt deformation and the formation of salt structures and associated rim synclines (Fig. 2; Lohr *et al.* 2007; Pharaoh *et al.* 2010). Phases of salt-tectonic activity vary regionally and reflect the tectonic evolution of the North German Basin (Urai *et al.* 2008; Pharaoh *et al.* 2010; Maystrenko *et al.* 2013; Warsitzka *et al.* 2019). Initial salt mobilization was triggered by Early to Middle Triassic extension. Subsequent extensional phases from the Late Triassic to Early Cretaceous caused further salt mobilization restricted to the tectonically active areas. Compression and basin inversion during the Late Cretaceous led to renewed salt mobilization throughout the basin. Cenozoic salt movement was related to regional extension or passive diapirism. Areas of intense Cenozoic salt movement include the West Schleswig Block, West and East Holstein Troughs, Glückstadt Graben and parts of the Mecklenburg and Prignitz Basins (Urai *et al.* 2008; Maystrenko *et al.* 2013; Warsitzka *et al.* 2019; Ahlrichs *et al.* 2021). Pleistocene and Holocene salt movement may be a continuation of the late Cenozoic trend or have been triggered or amplified by ice-sheet loading during the Pleistocene glaciations (Al Hseinat & Hübscher 2014; Lang *et al.* 2014; Al Hseinat *et al.* 2016; Huster *et al.* 2020; Hardt *et al.* 2021, 2024; Lang & Hampel 2023).

Pleistocene glaciations

From the Miocene, deposition in the study area was dominated by the Baltic River System, including its tributaries and westwards prograding delta (Bijlsma 1981; Thöle *et al.* 2014). The Baltic River System was shut down at the end of the Early Pleistocene, probably owing to glacial erosion in the source area (Bijlsma 1981). Since the Middle Pleistocene, the study area has been repeatedly overridden by the Fennoscandian Ice Sheet with the Middle Pleistocene Elsterian and Saalian and the Late Pleistocene Weichselian glaciations representing the major glacial stages (Fig. 1; Litt *et al.* 2007; Ehlers *et al.* 2011). The age and extent of earlier pre-Elsterian ice advances into the study area are poorly constrained. Tentative reconstructions suggest an east–west-directed ice advance that covered parts of northern Germany and the southeastern North Sea and may have occurred during Marine Isotopic Stage (MIS) 16 (Winsemann *et al.* 2020; Lohrberg *et al.* 2022a). The oldest well-documented ice advance that completely overrode the study area occurred during the Elsterian glaciation (Fig. 1; Ehlers *et al.* 2011). Glacigenic deposits, the provenance of erratic clasts and ice-advance directions indicate that two major ice advances occurred during the Elsterian glaciation (Eissmann 2002; Lang *et al.* 2012; Roskosch *et al.* 2015). The Elsterian glaciation is correlated with MIS 12 (Toucanne *et al.* 2009; Roskosch *et al.* 2015; Lauer & Weiss 2018; Arias *et al.* 2023). However, there is also evidence of a younger ice advance attributed to the Elsterian glaciation during MIS 10 (Litt *et al.* 2007; Roskosch *et al.* 2015). The Elsterian glaciation was followed by the Holsteinian interglacial (Litt *et al.* 2007; Ehlers *et al.* 2011).

The Saalian Complex was characterized by a long phase of fluctuating climate, while ice advances into the study area occurred only at the end of the Saalian Complex (Eissmann 2002; Litt *et al.* 2007). Indications of early Saalian ice advances during MIS 8 into the study area are considered uncertain (Roskosch *et al.* 2015; Lang *et al.* 2018). The late Saalian ice sheets again completely overrode the study area (Fig. 1). Three major ice advances are known from the older Saalian Drenthe stage that differ in ice-advance direction and maximum extent (Lang *et al.* 2018). The two major ice advances of the younger Saalian Warthe stage had a lesser maximum extents (Winsemann *et al.* 2020). Both the Drenthe and Warthe stages of the Saalian glaciation occurred during MIS 6 (Lüthgens *et al.* 2010; Roskosch *et al.* 2015; Lang *et al.* 2018). The Saalian glaciation was followed by the Eemian interglacial (Litt *et al.* 2007; Ehlers *et al.* 2011).

During the Late Pleistocene Weichselian, only the northern and eastern parts of the study area were glaciated (Fig. 1). At least four major ice advances are known that occurred during MIS 3 and MIS 2 (Litt *et al.* 2007; Lüthgens *et al.* 2020). However, recent studies suggest that the maximum extents of these ice advances are highly diachronous and reflect the dynamics of ice streams and lobes (Hughes *et al.* 2016; Patton *et al.* 2016; Lüthgens *et al.* 2020).

Tunnel-valley formation in the North German Basin

Buried and open Pleistocene tunnel valleys are a characteristic feature of the North German Basin and adjacent areas (Fig. 1; Hinsch 1979; Kuster & Meyer 1979; Ehlers *et al.* 1984; Ehlers & Linke 1989; Piotrowski 1994; Eissmann 2002; Lutz *et al.* 2009; Stackebrandt 2009; Lang *et al.* 2012; Lohrberg *et al.* 2020, 2022b; Breuer *et al.* 2023b; Gegg & Preusser 2023). The erosional base of the Middle Pleistocene tunnel valleys is commonly referred to as the base of the Pleistocene or Quaternary, respectively (Litt *et al.* 2007; Stackebrandt 2009; Breuer *et al.* 2023b). The preservation of older Pleistocene deposits is patchy (Litt *et al.* 2007), except within the deeper parts of the North Sea basin (Arfai *et al.* 2018). Based on the depositional architecture and lithostratigraphic criteria the Middle Pleistocene Elsterian glaciation is generally considered as the main phase of tunnel-valley formation (Kuster & Meyer 1979; Ehlers & Linke 1989; Eissmann 2002; Stackebrandt 2009; Winsemann *et al.* 2020). Post-glacial deposits in the upper parts of the tunnel-valley fills commonly include Holsteinian interglacial deposits, which provide an upper age boundary (Ehlers & Linke 1989; Eissmann 2002; Lang *et al.* 2012). However, numerical ages from the glacigenic

15023085, 0, Downloaded from https://onlinelibrary.wiley.com/doi/10.1111/bor.12694 by Rwth Aachen University Universitatsbibliothek- 021000, Wiley Online Library on [27/01/2025]. See the Terms and Conditions (https://onlinelibrary.wiley.com/terms-and-conditions) on Wiley Online Library for rules of use; OA articles are governed by the applicable Creative Commons License

infill of deep tunnel valleys are lacking. The Elsterian tunnel valleys are 3–5 km wide, can be more than 100 km long and are typically 300–400 m deep (Stackebrandt 2009; Kehew *et al*. 2012). The maximum known depth of an Elsterian tunnel valley is ~550 m b.s.l. (Schulz 2002). Very few tunnel valleys in the study area are attributed to the Saalian glaciation. Saalian tunnel valleys are generally much smaller than their Elsterian counterparts (<50 m deep, <1 km wide; Ehlers *et al*. 1984; Piotrowski *et al*. 1999; Passchier *et al*. 2010). Weichselian tunnel valleys are common in the study area and are 10–80 m deep, 0.5–1.5 km wide and several kilometres long (Smed 1998; Brose 2005). Underfilled Weichselian tunnel valleys form notable topographic valleys near the former ice margins. The dimensions and locations suggest an ice-marginal formation of these tunnel valleys (Smed 1998; Kehew *et al*. 2012).

Database and methods

This study makes use of an extensive database that is available on the geology of the North German Basin (onshore and offshore). For data compilation, visualization and analysis ArcGIS (version 10.8.2) and SKUA-GOCAD (version 22) were used.

Database

Tunnel valleys. – Maps of the tunnel valleys in the study area have been produced since the 1970s (e.g. Hinsch 1979; Kuster & Meyer 1979) and have continuously been updated. Data on the tunnel valleys generally comprise contour lines and are published as maps or parts of 3D subsurface models, respectively. A detailed description of the data of the state geological surveys was provided by Breuer *et al*. (2023a). Different input data have been used for mapping the tunnel valleys. In the western part of the study area, the mapping was mostly based on borehole data, while in the eastern and offshore parts of the study area, 2D seismic sections were the primary data source (Hönemann *et al*. 1995; Lutz *et al*. 2009; Stackebrandt 2009). A consequence of these different approaches is that mapped tunnel valleys appear broader in the eastern and narrower in the western regions of the study area (Fig. 1).

An updated overview map of the buried tunnel valleys in northern Germany was compiled by Breuer *et al*. (2023a, b) based on data sets provided by the state geological surveys (Table 1). Only tunnel valleys deeper than 100 m b.s.l. were considered for further analysis. In the existing data sets, tunnel valleys shallower than 100 m b.s.l. cannot be clearly identified. Breuer *et al*. (2023a, b) developed a GIS workflow to generate a map that is focused rather on the tunnel-valley network than on individual tunnel valleys. The tunnel-valley network was extracted using ArcGIS surface analysis and hydrology tools, providing a comprehensive map of tunnel-valley courses and depths (Breuer *et al*. 2023a, b). The extracted network of the onshore tunnel valleys has been used for the analysis presented in this study. Data on tunnel valleys in the German sector of the North Sea were compiled from Schwarz (1996), Lutz *et al*. (2009), Hepp *et al*. (2012) and Lohrberg *et al*. (2022b). For the North Sea, the available data are restricted to the tunnel-valley courses, while depth data are sparse (e.g. Lohrberg *et al*. 2022b). Additional data sets were created that comprise only tunnel-valley segments deeper than 200 m b.s.l. or located immediately above salt structures.

Faults and salt structures. – Faults and salt structures in the study area have been mapped based on the available borehole data and (generally 2D) seismic sections. The data have been published as maps (Brückner-Röhling *et al*. 2002, 2004; Reinhold *et al*. 2008; Warsitzka *et al*. 2019; Van Gessel *et al*. 2021), horizon maps (InSpEE 2015) and 3D subsurface models (BGR *et al*. 2022).

Fault trends were compiled from Brückner-Röhling *et al*. (2002, 2004), Ludwig & Stackebrandt (2010), Van Gessel *et al*. (2021) and BGR *et al*. (2022) (cf. Table 1, Figs 3, 4). For faults with available depth data, additional data sets were created that include only faults or segments of faults above depths of 1000 m b.s.l. The classification of faults as Palaeozoic (i.e. sub-salt) or Mesozoic and Cenozoic (i.e. supra-salt), respectively, does not necessarily imply the age of the fault, but refers to the stratigraphic unit where the fault displacement was mapped. Trends of the faults with the youngest phase of activity were plotted depending on the data availability (Table 1).

Data on salt structures were compiled from Reinhold *et al*. (2008), InSpEE (2015) and Warsitzka *et al*. (2019) (cf. Table 1, Figs 2–4). The orientations of the long axes of elongate salt structures were mapped in ArcGIS. The distinction between salt diapirs and salt pillows was adopted from Reinhold *et al*. (2008). Salt pillows have concordant contacts with the overburden, while salt diapirs have pierced parts of their overburden. A data set of shallow salt structures was created, which includes all salt structures that culminate above 1000 m b.s.l. All faults in the Mesozoic and Cenozoic successions located immediately above salt structures are regarded as crestal faults.

Uncertainties of the analysed data. – In general, the available data sets and maps have a high quality and the data density is high. For the tunnel-valley network, currently no harmonized map exists and small discontinuities may occur at state borders owing to the use of different data types and mapping approaches. Such discontinuities typically lead to sudden changes in the depth or width, while the tunnel valley courses are generally not affected. In contrast, the data sets on faults

15023885, 0, Downloaded from https://onlinelibrary.wiley.com/doi/10.1111/bor.12694 by Rwth Aachen University Universitatsbibliothek- 021000, Wiley Online Library on [27/01/2025]. See the Terms and Conditions (https://onlinelibrary.wiley.com/terms-and-conditions) on Wiley Online Library for rules of use; OA articles are governed by the applicable Creative Commons License

Table 1. Number of data points and sources used to plot the orientations of tunnel valleys, faults and salt structures.

			Region								
			North Sea	Pompeckj Block	Glückstadt Graben	Mecklenburg Basin	Grimmen and Rügen Highs	Altmark–Fläming Basin	Prignitz Basin	Lusatian Block	East Brandenburg Basin
Tunnel valleys	Number of datapoints in rose diagrams	All tunnel valleys	4591	15 567	12 125	17 520	1858	4184	19 479	5146	3721
		Deeper 200 m b.s.l.	n/a	2594	3036	2501	n/a	518	4065	1523	250
		Above salt structures	814	5072	3863	4407	63	925	3882	696	408
	Source		Schwarz (1996), Lutz *et al.* (2009), Hepp *et al.* (2012), Lohrberg *et al.* (2022b)	Breuer *et al.* (2023b)	Breuer *et al.* (2023b)	Breuer *et al.* (2023b)	Breuer *et al.* (2023b)	Jagemann & Müller (2023)	Breuer *et al.* (2023b)	Breuer *et al.* (2023b)	Breuer *et al.* (2023b)
Faults	Number of datapoints in rose diagrams	Active Neogene to Quaternary	3432[1]	1018	980	1848	460	n/a	378	851	416
		Active Miocene	1557[1]	2192	1209	n/a	n/a	n/a	n/a	n/a	n/a
		Active Palaeogene	[2]	[2]	[2]	n/a	[2]	1918	n/a	n/a	n/a
	Source		Brückner-Röhling *et al.* (2002, 2004)	Brückner-Röhling *et al.* (2002, 2004)	Brückner-Röhling *et al.* (2002, 2004)	Brückner-Röhling *et al.* (2002, 2004), LUNG MV (2023)	LUNG MV (2023)	Brückner-Röhling *et al.* (2002, 2004)	Ludwig & Stackebrandt (2010)	Ludwig & Stackebrandt (2010)	Ludwig & Stackebrandt (2010)
	Number of data points in rose diagrams	Cenozoic and Mesozoic (all)	160 286	157 843	53 526	20 740	5465	61 729	43 978	13 337	20 396
		Cenozoic and Mesozoic (above 1000 m b.s.l.)	20 761	36 952	16 773	7837	1638	19 439	11 921	4214	8375
		Crestal faults	27 940	10 534	8311	5403	255	3912	3301	323	735
	Source		BGR *et al.* (2022)	BGR *et al.* (2022)	BGR *et al.* (2022)	BGR *et al.* (2022)	BGR *et al.* (2022)	BGR *et al.* (2022)	BGR *et al.* (2022)	BGR *et al.* (2022)	BGR *et al.* (2022)
	Number of datapoints in rose diagrams	Palaeozoic	8409	18 654	4188	13 128	1273	7790	9680	2306	756
	Source		Brückner-Röhling *et al.* (2002, 2004)	Brückner-Röhling *et al.* (2002, 2004)	Brückner-Röhling *et al.* (2002, 2004)	BGR *et al.* (2022)	BGR *et al.* (2022)	Van Gessel (2021)	Van Gessel (2021)	Van Gessel (2021)	Van Gessel (2021)

(continued)

15023885, 0, Downloaded from https://onlinelibrary.wiley.com/doi/10.1111/bor.12694 by Rwth Aachen University Universitatsbibliothek- 021000, Wiley Online Library on [27/01/2025]. See the Terms and Conditions (https://onlinelibrary.wiley.com/terms-and-conditions) on Wiley Online Library for rules of use; OA articles are governed by the applicable Creative Commons License

Table 1. (continued)

		Region								
		North Sea	Pompeckj Block	Glückstadt Graben	Mecklenburg Basin	Grimmen and Rügen Highs	Altmark–Fläming Basin	Prignitz Basin	Lusatian Block	East Brandenburg Basin
Salt structures	Number of datapoints in rose diagrams	Salt diapirs	1944	2492	1945	200	n/a	437	241	16	n/a
		Salt pillows	1158	708	345	1325	70	480	1365	336	257
		Shallow salt structures	425	1642	1656	211	n/a	380	239	97	n/a
	Source		Reinhold *et al.* (2008), Doornenbal & Stevenson (2010), Warsitzka *et al.* (2019)	Reinhold *et al.* (2008), Doornenbal & Stevenson (2010), Warsitzka *et al.* (2019)	Reinhold *et al.* (2008), Doornenbal & Stevenson (2010), Warsitzka *et al.* (2019)	Reinhold *et al.* (2008), Doornenbal & Stevenson (2010), Warsitzka *et al.* (2019)	Reinhold *et al.* (2008), Doornenbal & Stevenson (2010), Warsitzka *et al.* (2019)	Reinhold *et al.* (2008), Doornenbal & Stevenson (2010), Warsitzka *et al.* (2019)	Reinhold *et al.* (2008), Doornenbal & Stevenson (2010), Warsitzka *et al.* (2019)	Reinhold *et al.* (2008), Doornenbal & Stevenson (2010), Warsitzka *et al.* (2019)

[1]Data compilations on young fault activity in the NW part of the German North Sea sector ('Duck's Beak') are not yet available.
[2]Trends of faults last active during the Palaeogene are only plotted if data on younger fault activity are not available.

and salt structures have been harmonized over larger areas to avoid such discontinuities.

A number of uncertainties are inherent to the analysed data sets. The data sets vary in scale and resolution and were produced for different objectives. Various types of input data were used to produce the maps and subsurface models. The data density, quality and resolution vary regionally and such variations are often no longer discernible in the published data sets. The original borehole and seismic data were mostly acquired for economic purposes (typically exploration and production of groundwater or hydrocarbons), leading to a concentration on specific regions and stratigraphic intervals. Uncertainties specific to seismic data include the resolution, processing and time-depth conversion. Seismic data used for the regional mapping are generally 2D sections and the line spacing limits the mapping resolution. Furthermore, all original data may have been affected by the subjectivity of the interpretations.

Methods

Regional subdivision. – The data sets were divided into nine regions, based on geological criteria and data availability (Figs 2–5). Regions represent structural elements such as fault-bounded blocks, sub-basins and structural highs of the Southern Permian Basin. The grouping by structural elements allows the analysis of the trends within regions of similar geological settings and history. The terminology and outlines of the structural elements are from Pharaoh *et al.* (2010). In some cases, several structural elements have been combined into one region, depending on geological similarity, data availability and size. Only faults and salt structures in the area where tunnel valleys attain maximum depths of more than 100 m b.s.l. were considered for further analysis (Fig. 1).

Data analysis. – Depth profiles were constructed for six tunnel valleys, using the tunnel-valley thalweg data and the tunnel-valley depth raster of Breuer *et al.* (2023b). The selected thalweg sections were manually retraced to extract topographic profiles using the ArcGIS '3D Analyst' toolbox. The six examples were selected based on the continuous data availability along the tunnel-valley courses. Along these profiles (Fig. 6), data were extracted from the stratigraphic units at the base of the tunnel valley (Doornenbal *et al.* 2010), the stratigraphic unit at a depth of 500 m b.s.l. (InSpEE 2015), and the locations of salt structures (InSpEE 2015). A Python script (version 3.10.12) was applied to extract the extents of stratigraphic units and salt structures along the profiles (Schützke 2024). The culmination depths of the salt structures were manually added to the profiles.

The trends of all tunnel valleys, faults and salt structures were plotted as rose diagrams for analysis and comparison (Figs 7–10). The vectors of the strikes of

15023885, 0, Downloaded from https://onlinelibrary.wiley.com/doi/10.1111/bor.12694 by Rwth Aachen University Universitatsbibliothek- 021000, Wiley Online Library on [27/01/2025]. See the Terms and Conditions (https://onlinelibrary.wiley.com/terms-and-conditions) on Wiley Online Library for rules of use; OA articles are governed by the applicable Creative Commons License

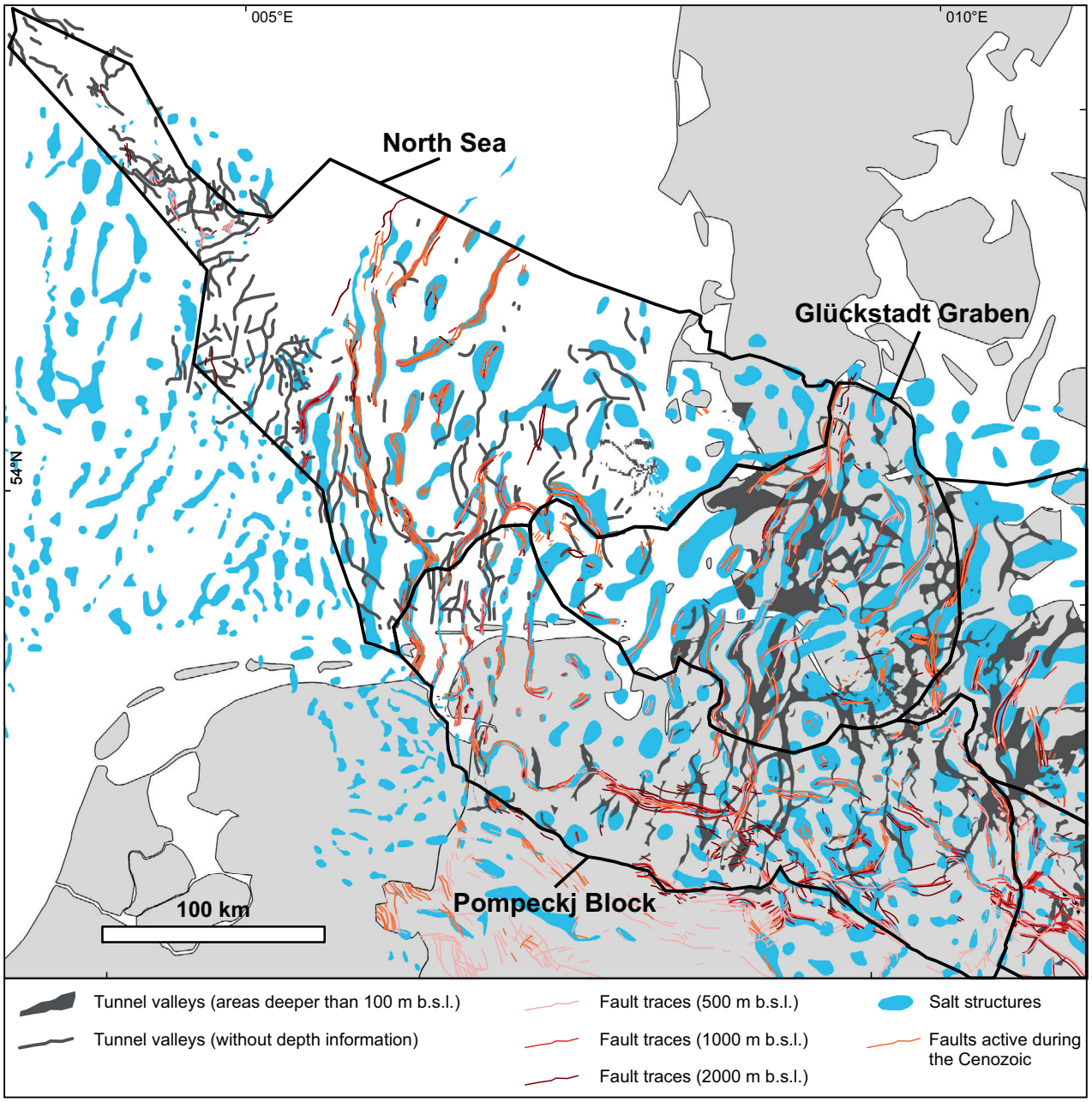

Fig. 3. Map of the western part of the study area, showing the analysed tunnel valleys (Lutz *et al.* 2009; Hepp *et al.* 2012; Lohrberg *et al.* 2022b; Breuer *et al.* 2023b), Mesozoic and Cenozoic faults (BGR *et al.* 2022) and salt structures (Reinhold *et al.* 2008; Warsitzka *et al.* 2019). Fault traces are plotted above tunnel valleys for better visibility.

all considered features were computed in SKUA-GOCAD. Prior to plotting, all line data were filtered to maximum segment lengths of 500 m to avoid distortion of the results by variations in segment lengths. Rose diagrams were plotted using the built-in Stereonet tool of SKUA-GOCAD. In the rose diagrams, the frequencies of the azimuth vectors were plotted symmetrically with petal widths of 10°. No further statistical analyses of the data were conducted owing to the inherent uncertainties of the data sets and to avoid overinterpretation. A summary of the results for each geological region is provided in Fig. 11.

Results

Basin geometry, basin fill and tunnel valleys

Plotting the tunnel valleys onto the thickness map of the Cenozoic succession (Fig. 5A) and the pre-Pleistocene subcrop map (Fig. 5B) provides an overview of the role of

15023085, 0, Downloaded from https://onlinelibrary.wiley.com/doi/10.1111/bor.12694 by Rwth Aachen University Universitatsbibliothek- 021000, Wiley Online Library on [27/01/2025]. See the Terms and Conditions (https://onlinelibrary.wiley.com/terms-and-conditions) on Wiley Online Library for rules of use; OA articles are governed by the applicable Creative Commons License

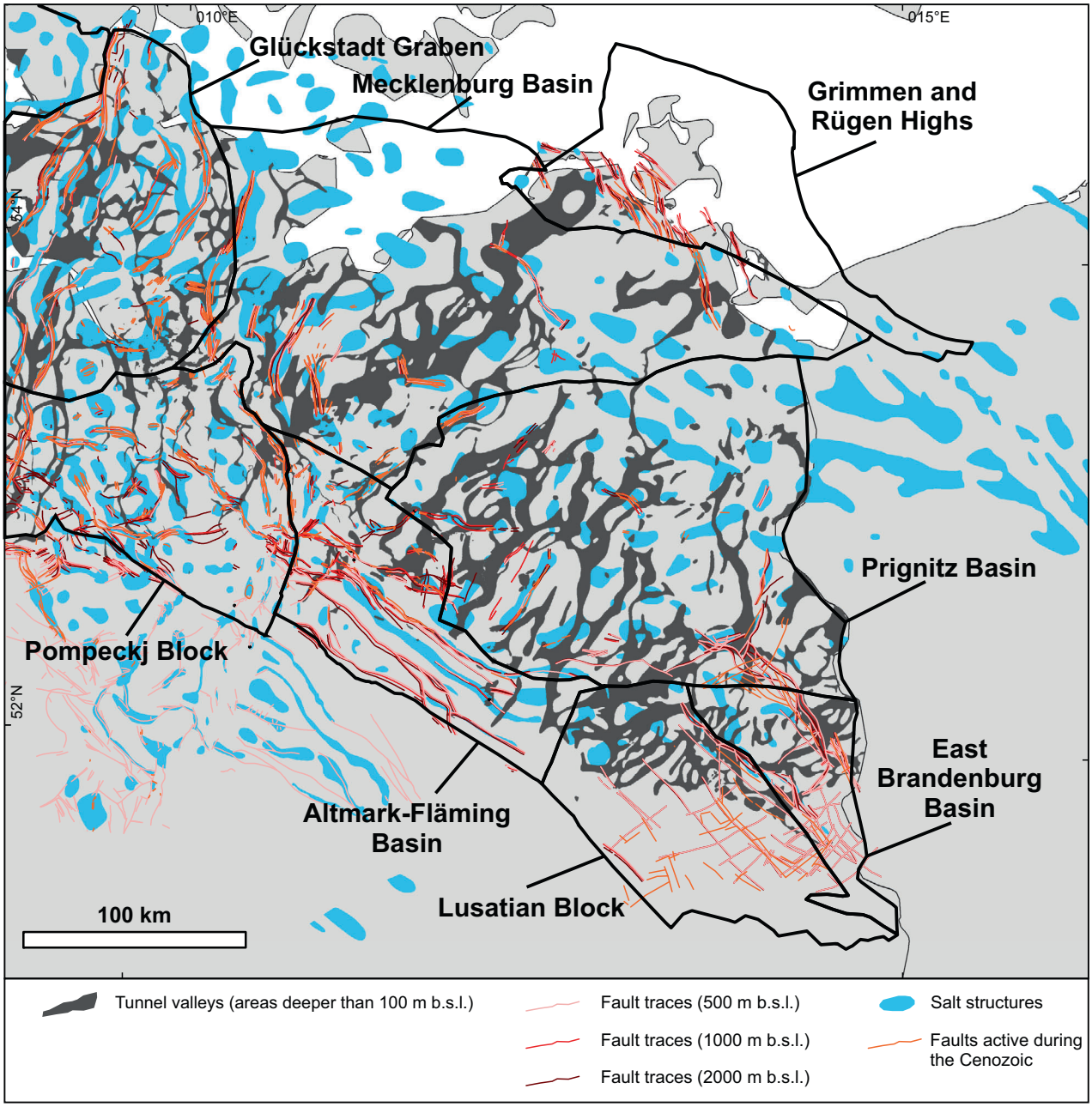

Fig. 4. Map of the eastern part of the study area, showing the analysed tunnel valleys (Jagemann & Müller 2023; Breuer *et al.* 2023b), Mesozoic and Cenozoic faults (BGR *et al.* 2022) and salt structures (Reinhold *et al.* 2008; Warsitzka *et al.* 2019). Fault traces are plotted above tunnel valleys for better visibility.

the regional basin geometry and fill on tunnel-valley distribution and depth. Tunnel valleys deeper than 100 m b.s.l. occur only along the axis of the North German Basin, where the Cenozoic succession is thick (Fig. 5A). Although the thickness of the Cenozoic succession decreases towards the SE, some very deep tunnel valleys (400–500 m b.s.l.) are present in the southeastern-most part of the study area (Lusatian Block and East Brandenburg Basin). However, tunnel valleys like these are incised in areas with an increased thickness of Cenozoic deposits in the vicinity of salt structures (Fig. 5A). The subcrop map and depth profiles show that deep tunnel valleys are restricted to those areas where the subsurface comprises Cenozoic, mostly Neogene, deposits (Figs 5B, 6). The Cenozoic succession in the study area consists of poorly consolidated terrestrial to shallow marine sand, silt and clay (Knox *et al.* 2010). Palaeogene deposits are incised by deep tunnel valleys in the southeastern part of the study area (Fig. 6F). Mesozoic rocks only subcrop the base of the

15023885, 0, Downloaded from https://onlinelibrary.wiley.com/doi/10.1111/bor.12694 by Rwth Aachen University Universitatsbibliothek- 021000, Wiley Online Library on [27/01/2025]. See the Terms and Conditions (https://onlinelibrary.wiley.com/terms-and-conditions) on Wiley Online Library for rules of use; OA articles are governed by the applicable Creative Commons License

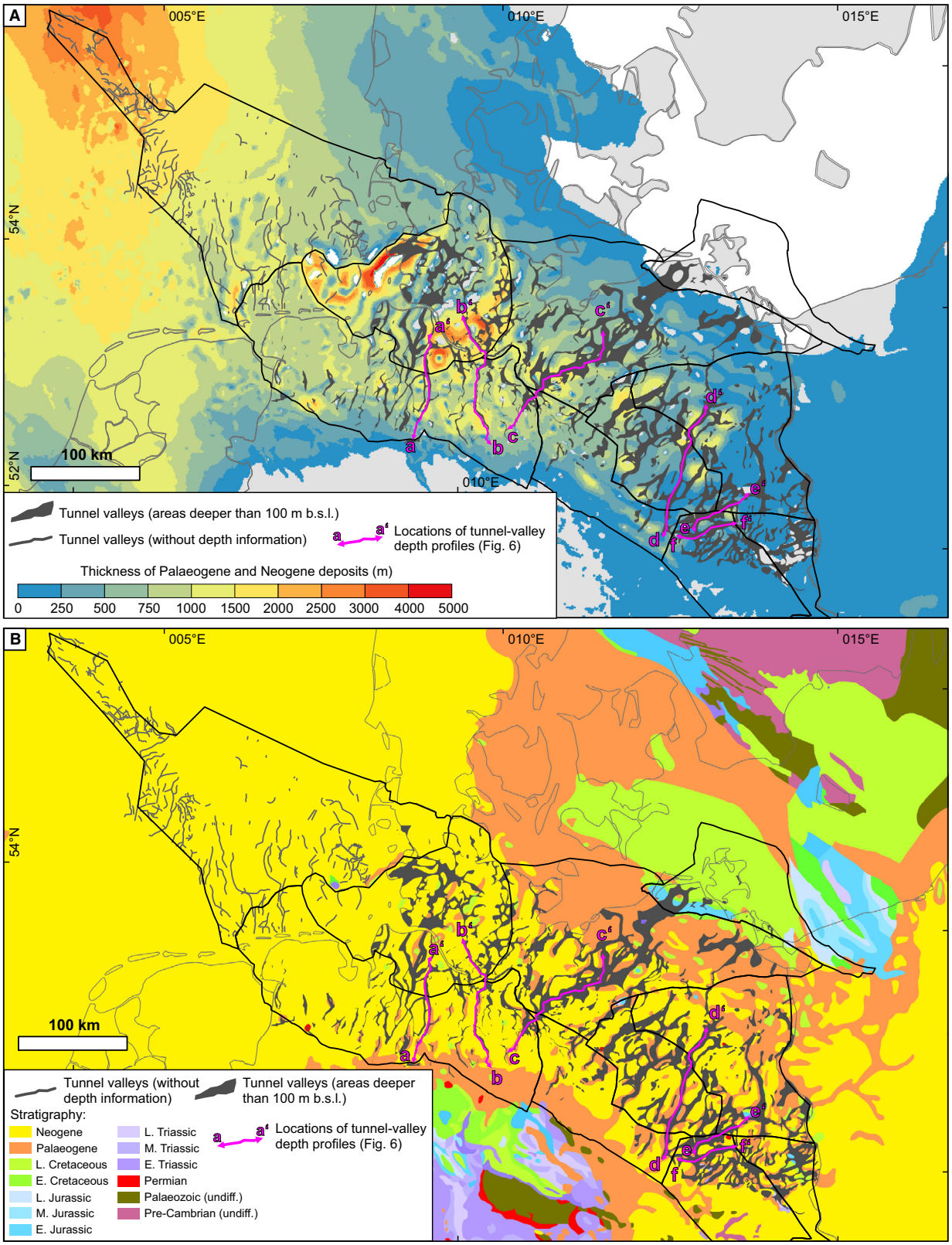

Fig. 5. Thickness map of the Cenozoic succession (Knox *et al.* 2010) (A) and pre-Quaternary subcrop map (Doornenbal *et al.* 2010) (B) of the study area. The locations and depths of tunnel valleys are from Lutz *et al.* (2009), Hepp *et al.* (2012), Lohrberg *et al.* (2022a, b), Breuer *et al.* (2023b) and Jagemann and Müller (2023). The black frames indicate the geological regions analysed in this study.

15023085, 0, Downloaded from https://onlinelibrary.wiley.com/doi/10.1111/bor.12694 by Rwth Aachen University Universitatsbibliothek- 021000, Wiley Online Library on [27/01/2025]. See the Terms and Conditions (https://onlinelibrary.wiley.com/terms-and-conditions) on Wiley Online Library for rules of use; OA articles are governed by the applicable Creative Commons License

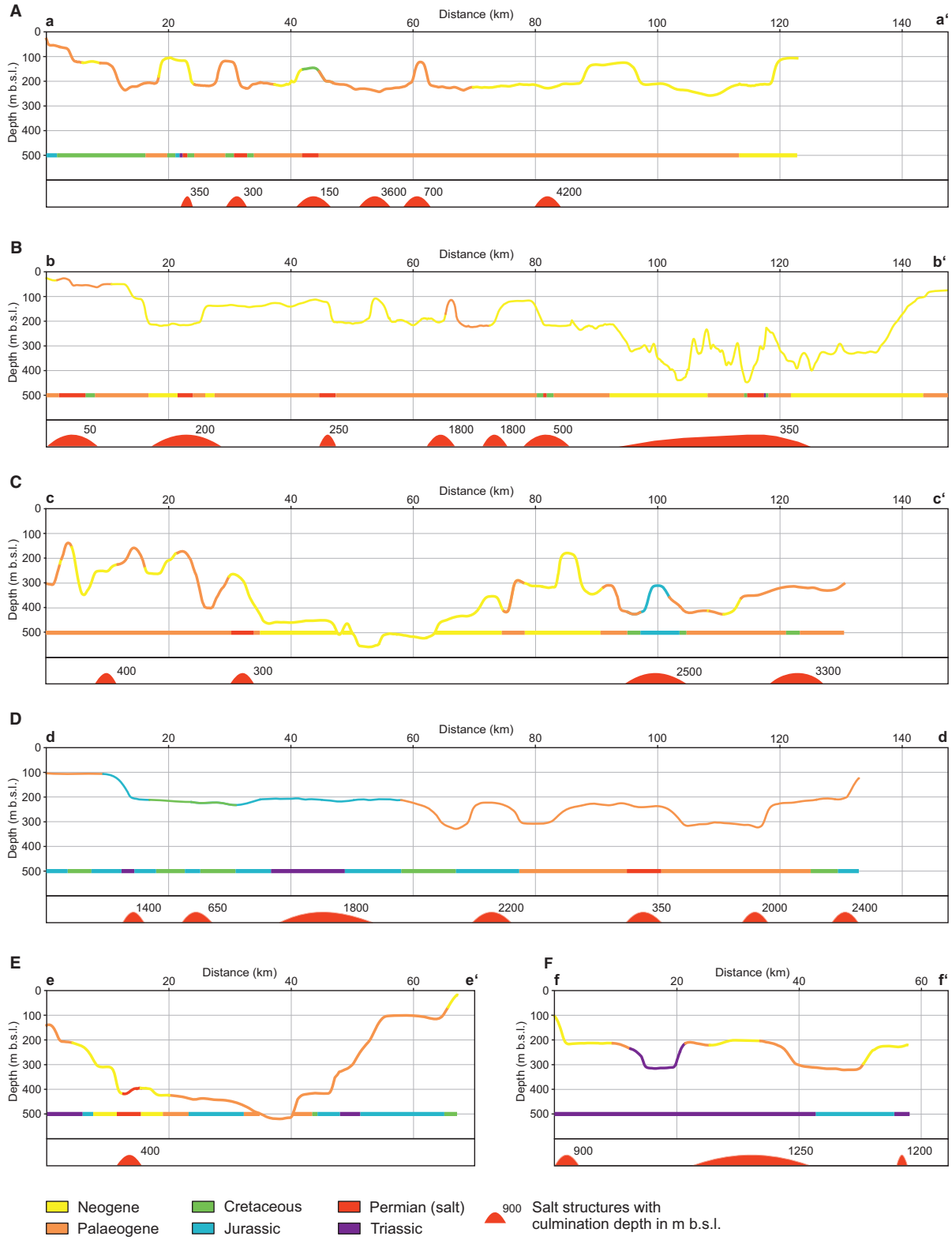

Fig. 6. A–F. Depth profiles along the thalwegs of selected tunnel valleys (locations are given in Fig. 5). The colours of the depth profiles indicate the stratigraphic units at the base of the tunnel valleys and were extracted from the pre-Quaternary subcrop map (Knox *et al.* 2010). The coloured bar indicates the stratigraphic unit in a depth of 500 m b.s.l. and was extracted from the corresponding horizon map (InSpEE 2015). Beneath each profile, the locations and culmination depths of salt structures are indicated (InSpEE 2015). Note that some mismatches between the stratigraphic units may occur owing to the different resolutions of the source maps.

15023885, 0, Downloaded from https://onlinelibrary.wiley.com/doi/10.1111/bor.12694 by Rwth Aachen University Universitatsbibliothek- 021000, Wiley Online Library on [27/01/2025]. See the Terms and Conditions (https://onlinelibrary.wiley.com/terms-and-conditions) on Wiley Online Library for rules of use; OA articles are governed by the applicable Creative Commons License

Pleistocene, if they were uplifted in the vicinity of salt structures (Fig. 5B). Along the depth profiles, Mesozoic rocks at or near the base of tunnel valleys tend to relate to highs (e.g. Fig. 6A, C, D). Salt structures crossed by tunnel valleys do not display a clear expression on the depth profiles of the tunnel valleys. Many salt structures leave no expression at all. Highs of the tunnel-valley base above salt structures may occur if Mesozoic rocks are present above the salt structure (e.g. Fig. 6A, C). *Vice versa*, lows may occur, if the tunnel-valley base is in direct contact with the salt structure (Fig. 6B, F).

Trends of tunnel valleys, faults and salt structures

North Sea. – The North Sea region comprises the Step Graben, Central Graben, Horn Graben, Schillgrund High and the West Schleswig Block (Figs 2, 3). The orientations of tunnel valleys, faults and salt structures in the North Sea region are all dominated by narrow north–south trends (Figs 7A–E, 8A–D). Shallow salt structures display NNW–SSE to NNE–SSW trends (Fig. 7E).

In summary, the North Sea region is characterized by a correlation between the orientations of tunnel valleys, faults and salt structures, which are all dominated by narrow north–south trends (Fig. 11).

Glückstadt Graben. – The Glückstadt Graben region comprises the Glückstadt Graben *sensu stricto* and the adjacent West and East Holstein Troughs (Figs 2, 3). In the Glückstadt Graben region, tunnel valleys display a dominant broad north–south and a secondary west–east trend (Fig. 7A). Tunnel-valley segments below 200 m b.s.l. display a broad north–south trend (Fig. 7B). Faults that were active during the Pliocene to Quaternary display a NNE–SSW trend (Fig. 7C). The Mesozoic and Cenozoic faults display a NNE–SSW trend, which is narrower for fault segments above 1000 m b.s.l. (Fig. 7D). Palaeozoic faults display a narrow NNE–SSW trend (Fig. 7E). Salt diapirs display a narrow NNE–SSW trend and salt pillows trend NE–SW (Fig. 8D). Shallow salt structures display narrow NNE–SSW trends (Fig. 8E). Crestal faults trend NNE–SSW (Fig. 8C). Tunnel-valley segments above salt structures display north–south to west–east trends (Fig. 8B).

In summary, in the Glückstadt Graben region a correlation between the orientations of faults, salt structures and the NNE–SSW-trending portion of the tunnel valleys is observed (Fig. 11).

Pompeckj Block. – In the Pompeckj Block region (Figs 2, 3), tunnel valleys and tunnel-valley segments below 200 m b.s.l. display narrow north–south trends (Fig. 7A, B). Faults that were active during the Pliocene to Quaternary display a narrow north–south trend (Fig. 7C). The Mesozoic and Cenozoic faults display a broad NW–SE trend (Fig. 7D). Palaeozoic faults display a narrow NNW–SSE trend (Fig. 7E). Salt diapirs display a dominant north–south trend and a secondary WNW–ESE trend. Salt pillows trend NNE–SSW (Fig. 8D). Shallow salt structures display a very broad NW–SE trend (Fig. 8E). Crestal faults trend broadly NW–SE (Fig. 8C). Tunnel-valley segments above salt structures display north–south to NW–SE trends (Fig. 8B).

In summary, in the Pompeckj Block region a correlation between the orientations of tunnel valleys and faults that were active during the Neogene to Quaternary can be observed, which is characterized by a narrow north–south trend. A correlation can also be observed between the orientations of tunnel valleys and salt structures, which are characterized by north–south trends (Fig. 11).

Mecklenburg Basin. – In the Mecklenburg Basin (Figs 2, 4), tunnel valleys and tunnel-valley segments below 200 m b.s.l. display a broad NE–SW trend (Fig. 7A, B). Faults that were active during the Palaeogene display a dominant narrow NNW–SSE and a secondary narrow west–east trend (Fig. 7C). The Mesozoic and Cenozoic faults display a narrow NNE–SSW trend (Fig. 7D). Palaeozoic faults display a narrow NNW–SSE trend (Fig. 7E). Salt diapirs trend NNW–SSE and salt pillows trend WNW–ESE. Both salt diapirs and salt pillows display a secondary NNE–SSW trend (Fig. 8D, E). Crestal faults narrowly trend NNE–SSW (Fig. 8C). Tunnel-valley segments above salt structures display NNE–SSW to ENE–WSW trends (Fig. 8B).

In summary, in the Mecklenburg Basin orientations of tunnel valleys correlate with the NNE–SSW trending Cenozoic and Mesozoic faults. Furthermore, the orientations of the tunnel valleys correlate with the secondary NNE–SSW trend of the salt structures and crestal faults (Fig. 11).

Grimmen and Rügen Highs. – In the Grimmen and Rügen Highs region (Figs 2, 4), tunnel valleys display a dominant north–south and a secondary ENE–WSW trend (Fig. 7A). No tunnel valleys deeper than 200 m b.s.l. are present in this area. Faults that were active during the Neogene to Quaternary display a narrow NW–SE trend (Fig. 7C). The Mesozoic and Cenozoic faults display a narrow NNW–SSE trend (Fig. 7D). The Palaeozoic faults trend NW–SE to WNW–ESE (Fig. 7D, E). Salt pillows and crestal faults display narrow NW–SE trends (Fig. 8C, D). No salt diapirs and shallow salt structures are present in this area. Tunnel valleys above salt pillows trend NNW–SSE, NNE–SSW and NW–SE (Fig. 8B).

In summary, in the Grimmen and Rügen Highs region no correlation between the orientations of tunnel valleys and faults is observed. A correlation occurs between the orientations of the secondary NNW–SSE trending tunnel-valley segments above salt pillows, salt pillows and crestal faults (Fig. 11).

15023085, 0, Downloaded from https://onlinelibrary.wiley.com/doi/10.1111/bor.12694 by Rwth Aachen University Universitatsbibliothek- 021000, Wiley Online Library on [27/01/2025]. See the Terms and Conditions (https://onlinelibrary.wiley.com/terms-and-conditions) on Wiley Online Library for rules of use; OA articles are governed by the applicable Creative Commons License

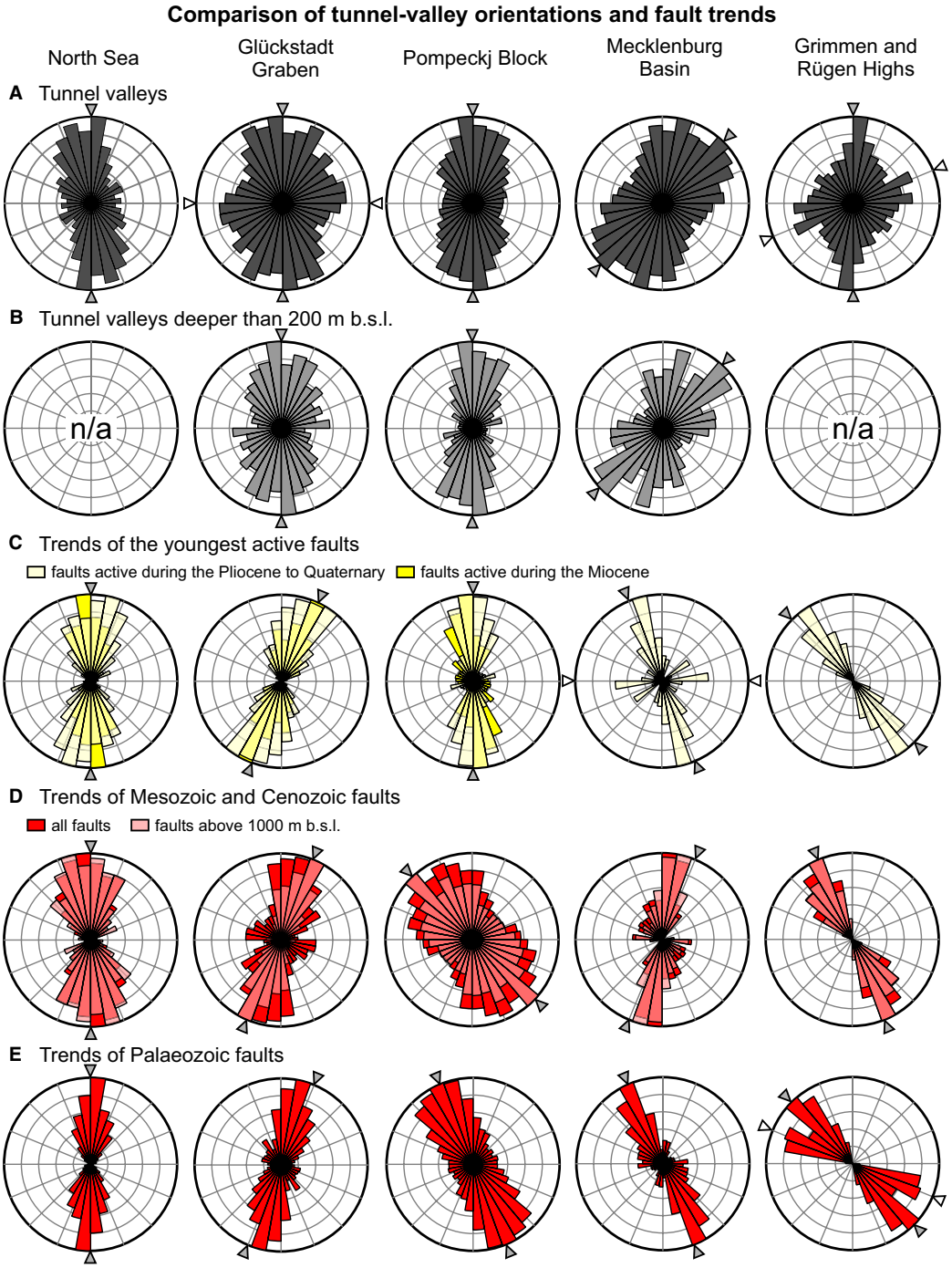

Fig. 7. Trends of tunnel valleys and faults in the western and northern parts of the North German Basin. The comparison reads vertically for each region. Dominant and secondary trends are indicated by grey and white triangles, respectively. The numbers and sources of data points used in each plot are given in Table 1. A. Trends of all tunnel valleys in the respective areas. B. Trends of tunnel-valley segments deeper than 200 m b.s.l. C. Trends of faults with the youngest phases of activity. The different colours indicate the age of the last phase of activity. D. Trends of faults within the Mesozoic and Cenozoic successions. The different colours distinguish all faults and fault segments above 1000 m b.s.l. E. Trends of tunnel-valley segments located immediately above salt structures.

Altmark–Fläming Basin. – In the Altmark–Fläming Basin (Figs 2, 4), tunnel valleys display a dominant north–south and a secondary west–east trend (Fig. 9A). Tunnel-valley segments below 200 m b.s.l. display NNE–SSW to north–south trends (Fig. 9B). Faults that were active during the Palaeogene display a dominant narrow NW–SE trend and secondary north–south to NE–SW trends (Fig. 9C). The Mesozoic and Cenozoic

15023885, 0, Downloaded from https://onlinelibrary.wiley.com/doi/10.1111/bor.12694 by Rwth Aachen University Universitatsbibliothek- 021000, Wiley Online Library on [27/01/2025]. See the Terms and Conditions (https://onlinelibrary.wiley.com/terms-and-conditions) on Wiley Online Library for rules of use; OA articles are governed by the applicable Creative Commons License

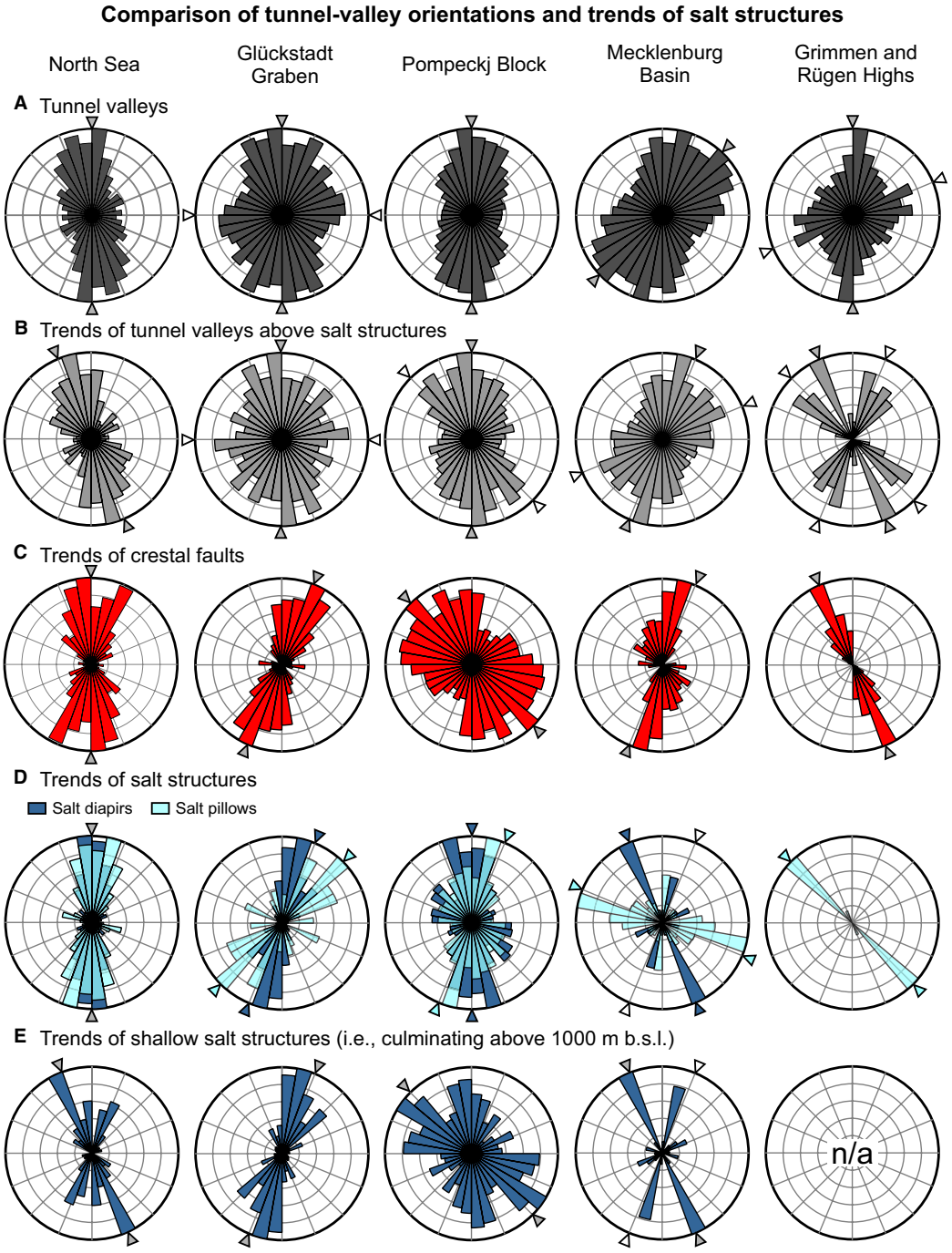

Fig. 8. Trends of tunnel valleys, crestal faults and salt structures in the western and northern parts of the North German Basin. The comparison reads vertically for each region. Dominant and secondary trends are indicated by grey and white triangles, respectively. Dominant trends of salt diapirs and pillows are indicated in the respective colour. The numbers and sources of data points used in each plot are given in Table 1. A. Trends of all tunnel valleys. B. Trends of tunnel-valley segments located immediately above salt structures. C. Trends of crestal faults. D. Trends of salt structures. The different colours indicate salt diapirs and salt pillows, respectively. E. Trends of shallow salt structures (i.e. salt structures culminating above 1000 m b.s.l.).

faults display a narrow WNW–ESE trend (Fig. 9D). The Palaeozoic faults display a narrow NW–SE trend (Fig. 9E). Salt diapirs and shallow salt structures trend WNW–ESE, NNE–SSW and west–east. Salt pillows display a narrow WNW–ESE trend (Fig. 10D, E). Crestal faults display a narrow WNW–ESE trend (Fig. 10C). Tunnel-valley segments above salt structures display north–south to west–east trends (Fig. 10B).

15023085, 0, Downloaded from https://onlinelibrary.wiley.com/doi/10.1111/bor.12694 by Rwth Aachen University Universitatsbibliothek- 021000, Wiley Online Library on [27/01/2025]. See the Terms and Conditions (https://onlinelibrary.wiley.com/terms-and-conditions) on Wiley Online Library for rules of use; OA articles are governed by the applicable Creative Commons License

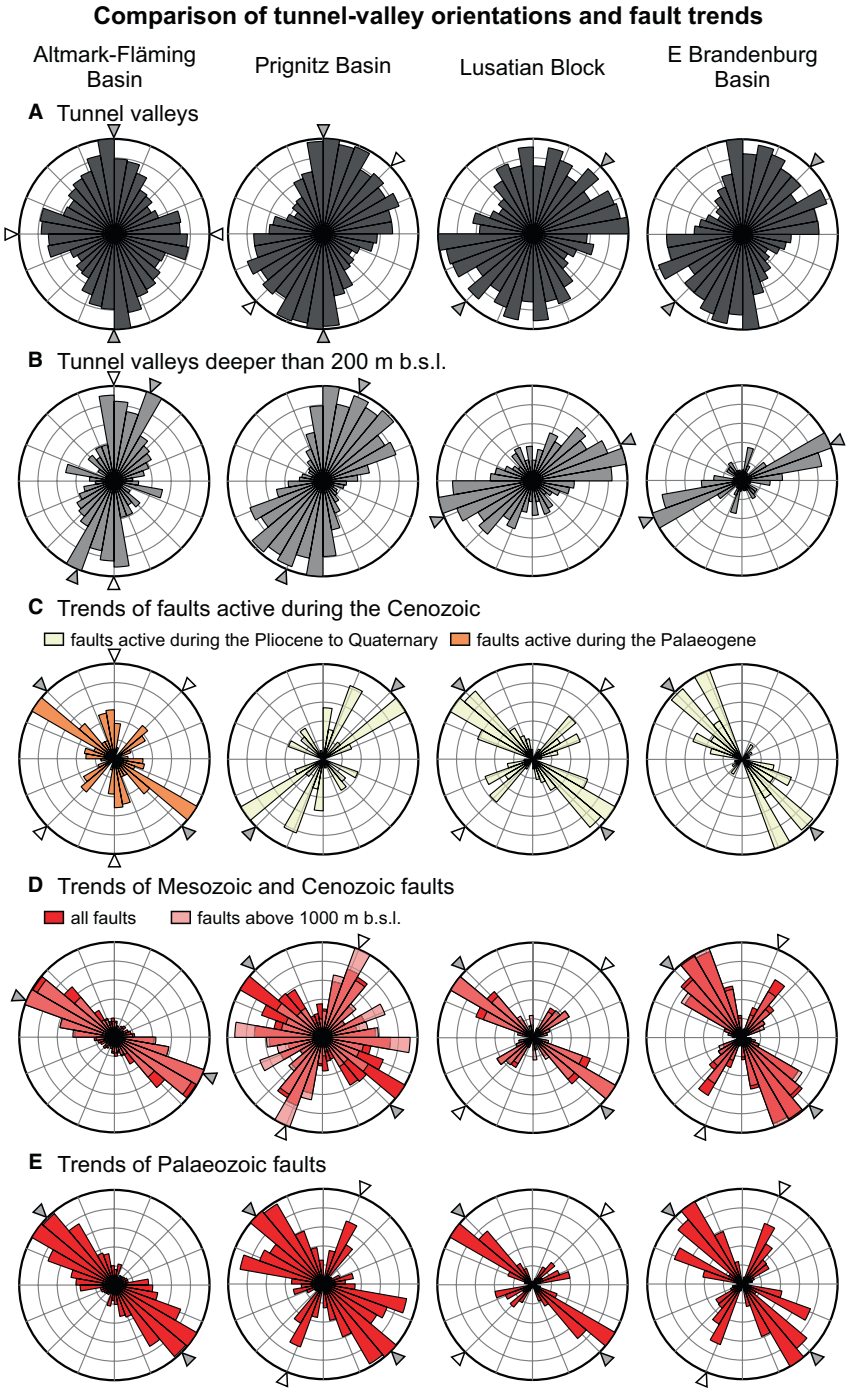

Fig. 9. Trends of tunnel valleys and faults in the eastern parts of the North German Basin. The comparison reads vertically for each region. Dominant and secondary trends are indicated by grey and white triangles, respectively. The numbers and sources of data points used in each plot are given in Table 1. A. Trends of all tunnel valleys in the respective areas. B. Trends of tunnel-valley segments deeper than 200 m b.s.l. C. Trends of faults with the youngest phases of activity. The different colours indicate the age of the last phase of activity. D. Trends of faults within the Mesozoic and Cenozoic successions. The different colours distinguish all faults and fault segments above 1000 m b.s.l. E. Trends of tunnel-valley segments located immediately above salt structures.

In summary, in the Altmark–Fläming Basin a correlation is observed between the orientations of parts of the tunnel valleys and the secondary NE–SW trend of faults last active during the Palaeogene and some salt diapirs (Fig. 11).

Prignitz Basin. – In the Prignitz Basin (Figs 2, 4), tunnel valleys display a broad NE–SW trend, showing a peak in the north–south direction (Fig. 9A). Tunnel-valley segments below 200 m b.s.l. trend broadly NNE–SSW (Fig. 9B). Faults that were active during the Pliocene to

15023085, 0, Downloaded from https://onlinelibrary.wiley.com/doi/10.1111/bor.12694 by Rwth Aachen University Universitatsbibliothek - 021000, Wiley Online Library on [27/01/2025]. See the Terms and Conditions (https://onlinelibrary.wiley.com/terms-and-conditions) on Wiley Online Library for rules of use; OA articles are governed by the applicable Creative Commons License

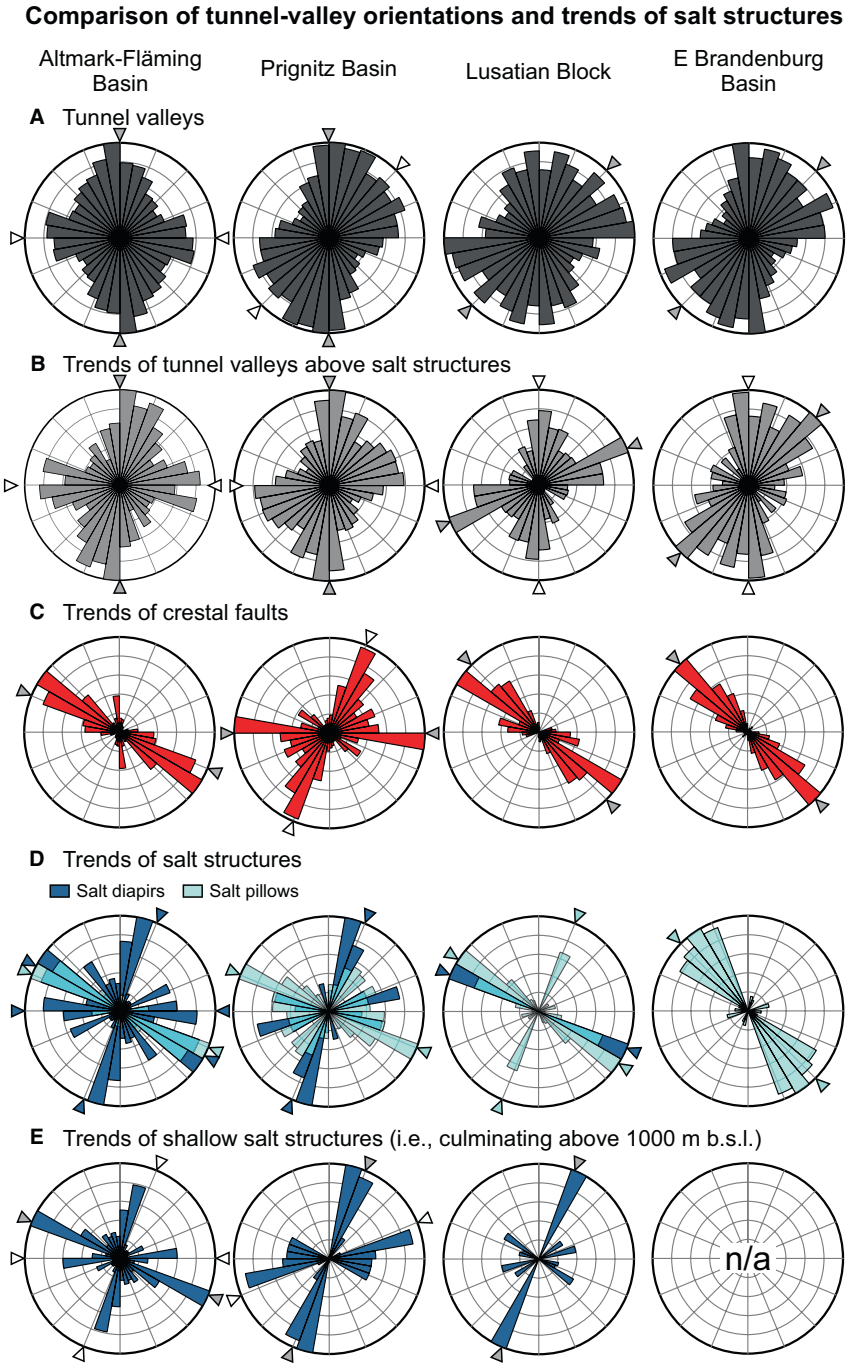

Fig. 10. Trends of tunnel valleys, crestal faults and salt structures in the eastern parts of the North German Basin. The comparison reads vertically for each region. Dominant and secondary trends are indicated by grey and white triangles, respectively. Dominant trends of salt diapirs and pillows are indicated in the respective colour. The numbers and sources of data points used in each plot are given in Table 1. A. Trends of all tunnel valleys. B. Trends of tunnel-valley segments located immediately above salt structures. C. Trends of crestal faults. D. Trends of salt structures. The different colours indicate salt diapirs and salt pillows, respectively. E. Trends of shallow salt structures (i.e. salt structures culminating above 1000 m b.s.l.).

Quaternary display a broad NW–SE trend (Fig. 9C). The Mesozoic and Cenozoic faults display a dominant NW–SE and a secondary NNE–SSW trend. Fault segments above 1000 m b.s.l. display a dominant NNE–SSW and a secondary west–east trend (Fig. 9D). Palaeozoic faults display a dominant broad NW–SE and a secondary NNE–SSW trend (Fig. 9E). Salt diapirs display a dominant NNE–SSW and a secondary ENE–WSW trend. Salt pillows display a dominant WNW–ESE and a secondary NNW–SSE trend (Fig. 10D). Shallow salt structures display a dominant NNE–SSW and a secondary ENE–WSW trend (Fig. 10E). Crestal

15023885, 0, Downloaded from https://onlinelibrary.wiley.com/doi/10.1111/bor.12694 by Rwth Aachen University Universitatsbibliothek - 021000, Wiley Online Library on [27/01/2025]. See the Terms and Conditions (https://onlinelibrary.wiley.com/terms-and-conditions) on Wiley Online Library for rules of use; OA articles are governed by the applicable Creative Commons License

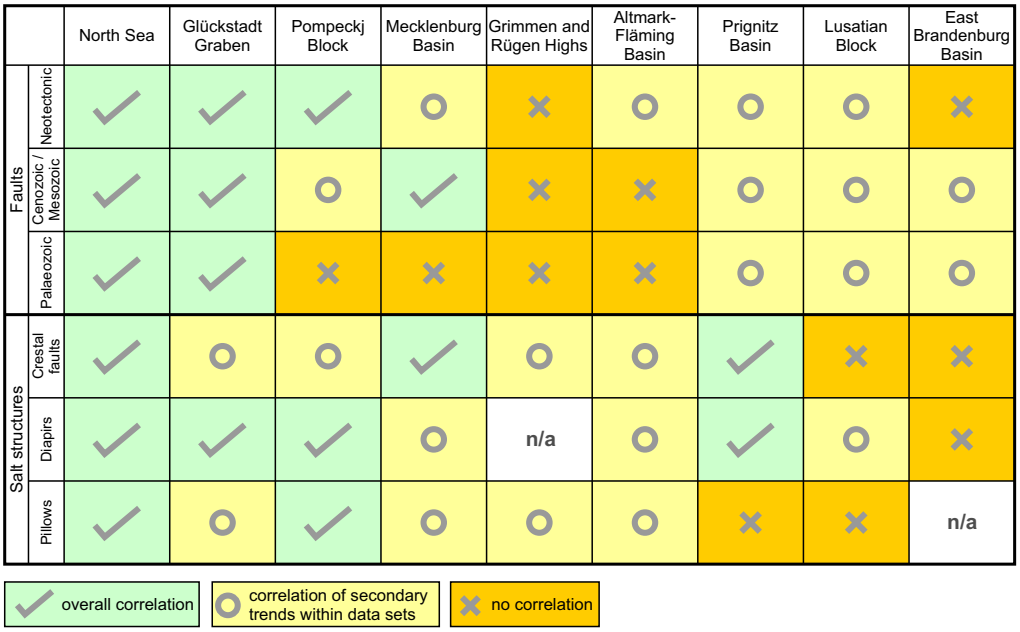

Fig. 11. Overview matrix of the correlations between the trends of tunnel valleys, faults and salt structures in the analysed geological regions.

faults display narrow west–east and NNE–SSW trends (Fig. 10C). Tunnel-valley segments above salt structures display a dominant north–south trend and a secondary trend west–east trend (Fig. 10B).

In summary, in the Prignitz Basin the orientations of tunnel valleys correlate with the NNE–SSW trending salt diapirs and crestal faults (Fig. 11). A correlation is also observed between the orientation of tunnel valleys and the secondary NNE–SSW trend of the faults, which is especially prominent for fault segments above 1000 m b.s.l.

Lusatian Block. – In the Lusatian Block region (Figs 2, 4), tunnel valleys very broadly trend NE–SW (Fig. 9A). Tunnel-valley segments below 200 m b.s.l. display a narrow ENE–WSW trend (Fig. 9B). Palaeozoic, Mesozoic and Cenozoic faults and faults that were active during the Pliocene to Quaternary display dominant NW–SE trends and secondary NE–SW trends (Fig. 9C–E). Salt structures narrowly trend NNW–SSE. Salt pillows display a secondary NNE–SSW trend (Fig. 10D). Shallow salt structures trend NNE–SSW (Fig. 10E). Crestal faults display a narrow NW–SE trend (Fig. 10C). Tunnel-valley segments above salt structures display a dominant ENE–WSW trend and a secondary north–south trend (Fig. 10B).

In summary, in the Lusatian Block region the orientations of tunnel valleys correlate with the secondary NE–SW trend of the faults (Fig. 11).

East Brandenburg Basin. – In the East Brandenburg Basin (Figs 2, 4), tunnel valleys very broadly trend NE–SW (Fig. 9A). Tunnel-valley segments below 200 m b.s.l. display a narrow ENE–WSW trend (Fig. 9B). Faults that were active during the Pliocene to Quaternary trend NW–SE (Fig. 9C). Palaeozoic, Mesozoic and Cenozoic faults display dominant NW–SE trends and secondary NNE–SSW trends (Fig. 9D, E). Salt pillows and crestal faults trend NW–SE (Fig. 10C, D). Tunnel-valley segments above salt structures trend north–south to NW–SE (Fig. 10B).

In summary, in the East Brandenburg Basin the orientations of tunnel valleys correlate with the secondary NNE–SSW trend of the faults (Fig. 11).

Interpretation and discussion

Distribution and orientation of tunnel valleys

The buried tunnel valleys in the North German Basin form a complex network, which presumably reflects the evolution of the Middle Pleistocene (Elsterian) ice sheets. Across the study area, the dominant trends of the tunnel valleys are north–south to NE–SW with north–south trends being more common in the western regions and NE–SW trends being more common in the eastern regions (Figs 7, 9). The orientations of tunnel valleys are considered to represent the main flow direction of subglacial meltwater, corresponding also to the ice-flow direction (Shreve 1972; Kehew *et al.* 2012; Kirkham *et al.* 2024b). Tunnel valleys are generally interpreted as structures forming when the ice sheet is in an overall recessive state (Kehew *et al.* 2012; Bjarnadóttir *et al.* 2017; Kirkham *et al.* 2024a). The presence of ice-flow-related subglacial landforms within tunnel-valley fills demonstrates that ice sheets are in a stage of dynamic

15023885, 0, Downloaded from https://onlinelibrary.wiley.com/doi/10.1111/bor.12694 by Rwth Aachen University Universitatsbibliothek- 021000, Wiley Online Library on [27/01/2025]. See the Terms and Conditions (https://onlinelibrary.wiley.com/terms-and-conditions) on Wiley Online Library for rules of use; OA articles are governed by the applicable Creative Commons License

retreat and not passively decaying during tunnel-valley incision (Kirkham *et al.* 2024a, b). Ice-flow directions interpreted from tunnel-valley trends may deviate from the ice-flow directions during the preceding advance phase of an ice sheet. The dominant trends of the buried tunnel valleys have been used to reconstruct the main ice-flow directions during the Middle Pleistocene Elsterian glaciation, which were from north to NE (Ehlers *et al.* 1984; Stackebrandt 2009). Other indicators for Elsterian ice-advance direction are rare (cf. Ehlers 1990; Ehlers *et al.* 2011), impeding the reconstruction of ice-sheet dynamics. Furthermore, an Elsterian origin of all buried tunnel valleys is not fully assured, as reliable dates for tunnel-valley formation and infilling are mostly lacking. In most regions analysed in this study, the orientations of the tunnel valleys display relatively broad variations. The tunnel-valley segments deeper than 200 m b.s.l. display narrower trends (Figs 7B, 9B) and allow for a clearer identification of the dominant directions. The orientations of these deep tunnel valleys can probably be considered as corresponding to the main ice-flow directions. Such larger tunnel valleys may represent major drainage pathways of the ice sheet that were active for extended periods. The (partial) reuse of existing tunnel valleys may also have contributed to the formation of the larger valleys and maintaining orientations over longer distances, as tunnel-valley fills may be easier to erode than the ambient substratum (Jørgensen & Sandersen 2006; Kristensen & Huuse 2012; Sandersen & Jørgensen 2012). Likewise, erosion by the ice flow may have contributed to the formation of the larger tunnel valleys (Jørgensen & Sandersen 2006; Kirkham *et al.* 2024a, b).

Secondary trends deviating from the dominant tunnel-valley trends can be clearly recognized from the maps and rose diagrams (Figs 1, 7, 9). Locally, tunnel valleys with such deviating trends have been the focus of more detailed studies (e.g. Hepp *et al.* 2012; Lohrberg *et al.* 2020, 2022b). Analyses of 3D seismic data sets from the central North Sea reveal multiple cross-cutting tunnel-valley generations, which probably derive from various glaciations and repeated ice-advances during these glaciations (Stewart & Lonergan 2011; Stewart *et al.* 2013; Ottesen *et al.* 2020; Kirkham *et al.* 2024b). Recent reconstructions of the Late Pleistocene Weichselian ice sheet reveal a highly dynamic pattern by complex lobes, multiple ice advances and ice streaming (Hughes *et al.* 2016; Lüthgens *et al.* 2020; Tylmann *et al.* 2022). By analogy, similar dynamics can be assumed for the Middle Pleistocene ice sheets, which would be reflected in the tunnel-valley network. Secondary tunnel-valley trends indicate variations of the ice-advance direction and probably the existence of multiple tunnel-valley generations, which may relate to distinct ice advances, changing ice-flow directions over the course of a glaciation or changes of the ice-margin configuration (Stewart & Lonergan 2011; Stewart *et al.* 2013; Ottesen *et al.* 2020; Kirkham *et al.* 2024b). The occurrence of cross-cutting tunnel-valley generations indicates that ice-sheet dynamics have the largest impact on tunnel-valley formation. This might even be considered as an argument against tunnel-valley reactivation and a control of structural features on tunnel-valley formation. Based on the data available for the study area, cross-cutting relationships and the relative age of the buried tunnel valleys cannot be resolved. It is likely that the apparent network of tunnel valleys is highly diachronous and actually represents multiple cross-cutting generations. Higher-resolution mapping of the distribution and orientations of tunnel valleys and the underlying substratum is necessary to identify tunnel-valley generations and assess controls on tunnel-valley incision.

The impact of the structural framework on tunnel-valley formation

The southern boundary of the area with tunnel valleys deeper than 100 m b.s.l. (Breuer *et al.* 2023b) provided a natural southern boundary of the analysed geological regions (Figs 3, 4). This observation affirms the control of the large-scale basin geometry and the presence of easily erodible deposits on tunnel-valley formation (cf. Boulton *et al.* 2009; Stackebrandt 2009; Breuer *et al.* 2023b). Shallower buried Elsterian tunnel valleys are known from the areas further south that were located closer to the maximum extents of the Elsterian ice sheets (e.g. Eissmann 2002; Lang *et al.* 2012). However, as no comprehensive map of these tunnel valleys exists they have not been included in our analysis.

Structural trends in the study area are characterized by NW–SE- to WNW–ESE-striking faults, which are aligned parallel to the basin margins, and NNW–SSE- to NE–SW-striking faults, which are aligned parallel to the major grabens and troughs that subdivide the North German Basin along its axis (Figs 7, 8; cf. Scheck *et al.* 2002; Lohr *et al.* 2007; Maystrenko *et al.* 2008; Pharaoh *et al.* 2010). The former dominate the southern and eastern regions of the study area, while the later dominate the northern and western regions of the study area. The occurrence of correlations between the orientations of tunnel valleys and faults varies strongly between the analysed regions (Fig. 11).

Correlations between the analysed features are common in the North Sea and Glückstadt Graben regions (Figs 7, 8, 11). Fault strikes in these regions display preferential north–south to NNE–SSW trends, while ice flow was probably from northerly directions (Ehlers *et al.* 1984, 2011; Ehlers 1990; Stackebrandt 2009). The matching directions may have enabled subglacial incision to exploit the existing structural weaknesses provided by the faults. In almost all other regions, correlations are only observed between secondary trends of the respective data sets (Fig. 11). These regions are all dominated by the NW–SE to WNW–ESE fault trend,

15023885, 0, Downloaded from https://onlinelibrary.wiley.com/doi/10.1111/bor.12694 by Rwth Aachen University Universitatsbibliothek- 021000, Wiley Online Library on [27/01/2025]. See the Terms and Conditions (https://onlinelibrary.wiley.com/terms-and-conditions) on Wiley Online Library for rules of use; OA articles are governed by the applicable Creative Commons License

which is hardly reflected in the tunnel-valley trends (Figs. 7, 9). If tunnel-valley orientations correlate with fault strikes, it is typically the secondary NNW–SSE to NE–SW trend. Ice advances in the eastern parts of the study generally were from NE to east directions (Eissmann 2002; Stackebrandt 2009). Therefore, an exploitation of existing structural weaknesses was probably only possible with the secondary fault trends. In summary, the analysis of the orientations suggests that correlations between tunnel-valley and fault trends occur only if fault trends match the general overall ice-flow direction. Ice advances during the Middle Pleistocene glaciations were directed from the sector stretching from NNW via north to east (e.g. Ehlers 1990; Eissmann 2002; Stackebrandt 2009; Lang *et al*. 2018). Faults with corresponding trends may have favoured incision, resulting in a correlation of tunnel-valley and fault trends.

When comparing the trends and locations of tunnel valleys and faults, it should be considered that the analysed faults represent rather large faults suitable for regional mapping (cf. BGR *et al*. 2022). In reality, faults actually represent fault-damage zones consisting of many smaller faults and fractures (Caine *et al*. 1996). Faults and fault-damage zones lower the resistance of rocks to erosion by fracturing and providing water-flow pathways (Molnar *et al*. 2007). However, as the near-surface infill of the North German Basin is dominated by unlithified siliciclastic rocks, the hydrogeological impact of faults is likely to have a greater impact than fracturing. In poorly lithified siliciclastic rocks, faults commonly form combined conduit–barrier systems with increased permeability along faults and decreased permeability across faults (Bense *et al*. 2013). Tunnel-valley incision is strongly affected by the interactions between the drainage of meltwater through subglacial conduits and aquifers. A sufficiently high permeability of the substratum will allow for meltwater drainage without the need to form tunnel valleys. *Vice versa*, incision is initiated if the capacity to drain the meltwater through aquifers is exceeded, e.g. in areas characterized by low-permeability rocks (Piotrowski 1997; Huuse & Lykke-Andersen 2000; Boulton *et al*. 2009; Sandersen & Jørgensen 2012). Once initiated, subglacial conduits act as sinks for meltwater draining through aquifers and become enlarged by additional meltwater inflow and sediment creep (Piotrowski *et al*. 1999; Boulton *et al*. 2009; Janszen *et al*. 2012). Insufficient drainage through either the conduits or the aquifers may lead to a build-up of overpressure, potentially triggering hydraulic fracturing, liquefaction or fluidization of the substratum, greatly enhancing tunnel-valley incision (Janszen *et al*. 2012; Ravier *et al*. 2014, 2015). Complex substrates with interbedded permeable and impermeable layers enhance the potential for the build-up of overpressure (Janszen *et al*. 2012; Ravier *et al*. 2014, 2015). Likewise, the modification of the permeability by faults will enhance the potential for subglacial incision (Wenau & Alves 2020).

Correlations between the trends of the youngest faults, crestal faults and tunnel valleys are common. These patterns can be expected as the youngest and uppermost faults are most likely to interact with Earth-surface processes. Neotectonically active faults have been interpreted as representing zones of weakness that are especially prone to tunnel-valley incision (Reicherter *et al*. 2005; Stackebrandt 2009; Brandes *et al*. 2022; Sandersen & Jørgensen 2022). In the study area, neotectonic faults include faults that have been active since the Oligocene (AkEnd 2002; Brückner-Röhling *et al*. 2004; Stackebrandt 2004), when the present-day stress field was first established (Kaiser *et al*. 2005; Reicherter *et al*. 2005). Other neotectonically active faults have been reactivated by glacial isostatic adjustment (Brandes *et al*. 2015, 2019; Müller *et al*. 2022). The analysed faults all belong to the former category (Brückner-Röhling *et al*. 2002, 2004; Ludwig & Stackebrandt 2010). The present-day stress field is fan-shaped with an orientation of the maximum horizontal stress (S_{Hmax}) of NNW–SSE to NE–SW (Marotta *et al*. 2002; Heidbach *et al*. 2018; Ahlers *et al*. 2022). The NW–SE to NE–SW strike of faults active during the Neogene and Quaternary (Figs 7, 9) relate to west–east-directed extension in the regional stress field (Maystrenko *et al*. 2005; Reicherter *et al*. 2005; Ahlrichs *et al*. 2021; Ahlers *et al*. 2022). The trends of the youngest active faults in most regions coincide with the trends of salt structures (Figs 7–10), supporting the interpretation that deep-rooted Neogene and Quaternary faulting in the study area is commonly related to salt structures (e.g. Brückner-Röhling *et al*. 2002; Al Hseinat *et al*. 2016; Arfai *et al*. 2018). The overall orientation of the tunnel valleys in the North German Basin conspicuously follows the regional stress field. Many of the youngest active faults are NNW–SSE- to NE–SW-trending normal faults (Brückner-Röhling *et al*. 2004; Ahlers *et al*. 2022), which were favourably aligned for Pleistocene tunnel-valley incision (Figs. 7, 9). The present-day regional stress field is further affected by glacial isostatic adjustment (GIA) and evidence of fault reactivation is known from a number of NW–SE- to WNW–ESE-striking faults (Brandes *et al*. 2015, 2019; Müller *et al*. 2022). The strike of the few mapped reactivated faults in the North German Basin is normal to oblique to the main ice-flow directions. Based on the available data, the impact of GIA on tunnel-valley incision was probably low. An amplification of movements along faults that were neotectonically active since the Oligocene by GIA cannot be excluded. However, GIA is not a requisite to explain young faulting in the study area and correlations between the orientations of young faults and tunnel valleys. Brandes *et al*. (2022) and Sandersen & Jørgensen (2022) argued that fault zones reactivated by GIA in northern Denmark are prone to erosion and

15023085, 0, Downloaded from https://onlinelibrary.wiley.com/doi/10.1111/bor.12694 by Rwth Aachen University Universitatsbibliothek- 021000, Wiley Online Library on [27/01/2025]. See the Terms and Conditions (https://onlinelibrary.wiley.com/terms-and-conditions) on Wiley Online Library for rules of use; OA articles are governed by the applicable Creative Commons License

tunnel-valley incision. The data from northern Denmark (Sandersen & Jørgensen 2022) suggest a much closer correlation between faults and tunnel valleys than the data from the North German Basin. The difference might be explained by a more favourable orientation of fault trends and ice-advance directions.

Correlations between the orientations of tunnel valleys and the trends of elongated salt structures are observed in some of the analysed regions and lacking in others (Fig. 11). As the trends of the salt structures generally follow the trends of the faults (Figs 7–10), correlations between the orientations of tunnel valleys and salt structures occur typically in the same regions as correlations between the orientations of tunnel valleys and faults. The close correlation of faults and salt structures illustrates the co-evolution of faults and salt structures, as all tectonic phases during the Mesozoic and Cenozoic triggered salt mobilization (Urai *et al*. 2008; Maystrenko *et al*. 2013; Warsitzka *et al*. 2019; Ahlrichs *et al*. 2021). The strikes of crestal faults follow the trends of salt structures but may locally diverge from the regional fault trends, as crestal faulting is primarily controlled by the rising salt structure, potentially decoupling crestal faulting from the regional stress field (Lohr *et al*. 2007). As with the fault trends, correlations between the orientations of tunnel valleys and salt structures are commonly observed if the trends of salt structures parallel the main ice-flow directions. Salt structures may favour the incision of tunnel valleys (cf. Huuse & Lykke-Andersen 2000; Lang *et al*. 2014; Wenau & Alves 2020) if they lack overlying resistant rocks (typically Mesozoic) and culminate close to surface (Fig. 6B; salt structure at ~115 km). Crestal faults may also favour incision, especially if their orientation parallels the ice-flow direction and they have been recently active. *Vice versa*, salt rise may have uplifted resistant rocks that hinder incision or created local topographic and hydrogeological conditions, deflecting the flow of ice and meltwater and thus shift incision away from the salt structure (Fig. 6F; salt structure at ~100 km) (Kuster & Meyer 1979; Piotrowski 1997; Kristensen *et al*. 2008). The presence of rim synclines filled by easily erodible deposits may also promote tunnel-valley incision (Piotrowski 1994; Lang *et al*. 2012). Because rim synclines usually parallel elongated salt structures, no separate analysis of their orientation was performed.

Robustness of the orientation data

The maps and subsurface models that were used to generate the orientation data are affected by a number of uncertainties that mainly relate to the density, quality and resolution of the input data. However, the data density in the study area is generally high. The North German Basin is an area with a long research history and both the maps of the tunnel valleys and the structural features have been continuously updated over decades (cf. Stackebrandt 2009; Müller *et al*. 2016; Breuer *et al*. 2023a, b). It is probably safe to assume that the data on the structural features are very robust and major uncertainties will only occur at higher resolutions that are beyond the scope of this study. For the tunnel valleys, the database is regionally more variable and available maps may suffer from data clustering or lacking in certain areas. However, the major tunnel valleys are well-constrained. Smaller tunnel valleys may be less well-constrained, especially if orientations deviate from the main trends. Here, the lack of high-resolution or 3D data has a large impact. Recent studies from the North Sea demonstrated that the tunnel-valley network is more complex than previously assumed when imaged in 3D seismic volumes (Stewart *et al*. 2013; Kirkham *et al*. 2021, 2024a, b) or densely spaced high-resolution 2D seismic sections (Lohrberg *et al*. 2020, 2022b).

The presented analysis should be considered as a basin- or regional-scale overview, similar to the work presented by Sandersen & Jørgensen (2022) for the Danish Basin. Higher-resolution, 3D data are needed to understand the impact of structural features on tunnel-valley formation on a more local scale, as in the work presented by Wenau & Alves (2020). Such studies should ideally also consider the lithology of the underlying strata (Janszen *et al*. 2012).

Assessing the potential for future tunnel-valley formation

In long-term safety assessments for radioactive waste repositories potential future glaciations and thus tunnel-valley formation have to be taken into account (Talbot 1999; Fischer *et al*. 2021). However, the dynamics of such future ice sheets are basically unpredictable. Knowing the impact of the underlying geology on subglacial incision can provide an idea of areas with an increased risk of subglacial incision and thus help in long-term safety assessments. By analogy, it can be assumed that potential future ice sheets in northern Europe will display similar dynamics as the Pleistocene ice sheets and ice-flow direction will be alike (cf. Fischer *et al*. 2021; Breuer *et al*. 2023b). Faults and elongated salt structures may become preferential pathways for incision and tunnel-valley formation if they trend NNW–SSE to west–east and thus parallel to potential ice-flow directions. Neotectonically active faults are also more likely to become sites of future incision and should thus be avoided in the site-selection process. With regard to potential future tunnel-valley formation that can impact the long-term safety of a radioactive waste repository, the presence and orientations of faults and salt structures do not provide consistent indicators for the locations of future incision. In poorly consolidated deposits such as the Cenozoic infill of the North German Basin faults are clearly not a prerequisite for erosion.

15023885, 0, Downloaded from https://onlinelibrary.wiley.com/doi/10.1111/bor.12694 by Rwth Aachen University Universitatsbibliothek- 021000, Wiley Online Library on [27/01/2025]. See the Terms and Conditions (https://onlinelibrary.wiley.com/terms-and-conditions) on Wiley Online Library for rules of use; OA articles are governed by the applicable Creative Commons License

Conclusions

The objective of this study was to improve the understanding of the impact of the structural framework on the formation, distribution and orientation of tunnel valleys. An extensive data set from the North German Basin, comprising tunnel valleys, faults, salt structures and the basin fill was analysed for this study. Three hypotheses on the impact of the geological structure of the subsurface on tunnel-valley formation were tested.

1 *Tunnel valleys are preferentially incised into those parts of sedimentary basins that contain thick successions of poorly consolidated and thus erodible deposits:* our analysis confirms that the regional distribution of buried tunnel valleys in the North German Basin is controlled by the overall basin geometry and the presence of erodible Cenozoic deposits. The southern boundary of the area with tunnel valleys deeper than 100 m b.s.l. provided a natural boundary, corresponding to the boundaries of large-scale structural elements of the North German Basin. The deepest tunnel valleys are always incised into Cenozoic, especially Neogene, deposits.
2 *Faults promote tunnel-valley incision and tunnel valleys align with faults, especially if these faults have been neotectonically active:* correlations between the orientations of tunnel valleys and faults are only observed in some regions or sub-sets of the analysed data, respectively. The analysis of the orientation data suggests that correlations between tunnel-valley and fault trends occur if fault trends match the main Pleistocene ice-flow directions (typically from the sector NNW via north to east). The orientations of tunnel valleys commonly follow the trends of faults in areas where regional fault trends are NNW–SSE to east–west and ice-advance directions were approximately parallel. However, correlations are rarely observed if the regional fault trend is NW–SE to WNW–ESE and ice advances occurred thus normal or oblique to the regional fault trend. The impact of faults on the evolution of the tunnel-valley network probably varied regionally. Faults active under the present-day stress field typically are NNW–SSE to NE–SW trending normal faults. Therefore, the strikes of neotectonically active faults are commonly favourable for tunnel-valley incision and may have promoted subglacial erosion.
3 *The presence of salt structures facilitates tunnel-valley incision:* no clear correlation between the orientations of tunnel valleys and elongated salt structures can be identified. As with the fault trends, correlations are commonly observed if the trends of salt structures parallel the main ice-flow directions. Incision above salt structures may be promoted if salt structures culminate near the surface and lack overlying resistant rocks. Conversely, the presence of resistant (typically Mesozoic) rocks above a salt structure may shift the incision away from the salt structure.

A major motivation for this study was the potential impact of future glaciations and tunnel-valley incision on the long-term safety of radioactive waste repositories. By analogy to the Pleistocene glaciations, future ice advances into the area of the North German Basin will display similar main ice-flow directions. Therefore, faults and salt structures that trend NNW–SSE to east-west may be more susceptible to incision owing to their potentially favourable orientation. Neotectonically active faults are also more likely to become sites of future incision and should thus be avoided in the site-selection process. However, the presence and orientation of faults and salt structures do not provide consistent indicators for the locations of future tunnel-valley incision.

Acknowledgements. – The state geological surveys of Berlin, Brandenburg, Bremen, Hamburg, Lower Saxony, Mecklenburg–Western Pomerania, Saxony–Anhalt and Schleswig–Holstein are gratefully acknowledged for providing maps and data. We thank AspenTech for providing SKUA-GOCAD licences via the Academic Software Program (https://www.aspentech.com/en/academic-program) to support BGR as a national geological service in non-profit work for the public and education. K. Fischer-Appelt and H. Stück are thanked for discussion. Constructive reviews by A. Lohrberg and P. Sandersen and editorial handling by J. A. Piotrowski are highly appreciated. The authors declare that they have no known competing financial or non-financial interests that could have appeared to influence the work reported in this paper. Open Access funding was provided by Projekt DEAL.

Author contributions. – JL: Design of the study; data compilation, analysis and interpretation; drawing of figures; writing of the manuscript. AB and VN: Contributions to the regional geology and the discussion. JS: Construction and analysis of the tunnel-valley depth profiles (as part of her BSc thesis). SW: Contributions to the discussion. SB: Data compilation, analysis and interpretation; contributions to the discussion. All authors have approved the submitted version of the manuscript.

Data availability statement. – The data that support the findings of this study are available from the cited published sources. Data compilations are available from the corresponding author upon reasonable request.

References

Ahlers, S., Röckel, L., Hergert, T., Reiter, K., Heidbach, O., Henk, A., Müller, B., Morawietz, S., Scheck-Wenderoth, M. & Anikiev, D. 2022: The crustal stress field of Germany: a refined prediction. *Geothermal Energy 10*, 10. https://doi.org/10.1186/s40517-022-00222-6.

Ahlrichs, N., Noack, V., Hübscher, C., Seidel, E., Warwel, A. & Kley, J. 2021: Impact of Late Cretaceous inversion and Cenozoic extension on salt structure growth in the Baltic sector of the North German Basin. *Basin Research 34*, 220–250. https://doi.org/10.1111/bre.12617.

AkEnd 2002: *Auswahlverfahren für Endlagerstandorte: Empfehlungen des AkEnd – Arbeitskreis Auswahlverfahren Endlagerstandorte*. 260 pp. Arbeitskreis Auswahlverfahren Endlagerstandorte, Köln.

Al Hseinat, M. & Hübscher, C. 2014: Ice-load induced tectonics controlled tunnel valley evolution – instances from the southwestern Baltic Sea. *Quaternary Science Reviews 97*, 121–135. https://doi.org/10.1016/j.quascirev.2014.05.011.

15023085, 0, Downloaded from https://onlinelibrary.wiley.com/doi/10.1111/bor.12694 by Rwth Aachen University Universitatsbibliothek- 021000, Wiley Online Library on [27/01/2025]. See the Terms and Conditions (https://onlinelibrary.wiley.com/terms-and-conditions) on Wiley Online Library for rules of use; OA articles are governed by the applicable Creative Commons License

Al Hseinat, M., Hübscher, C., Lang, J., Lüdmann, T., Ott, I. & Polom, U. 2016: Triassic to recent tectonic evolution of a crestal collapse graben above a salt-cored anticline in the Glückstadt Graben/North German Basin. *Tectonophysics 680*, 50–66. https://doi.org/10.1016/j.tecto.2016.05.008.

Arfai, J., Franke, D., Lutz, R., Reinhardt, L., Kley, J. & Gaedicke, C. 2018: Rapid quaternary subsidence in the northwestern German North Sea. *Scientific Reports 8*, 11524. https://doi.org/10.1038/s41598-018-29638-6.

Arias, S. F., Förster, M. W. & Sirocko, F. 2023: Rieden tephra layers in the Dottinger Maar lake sediments: implications for the dating of the Holsteinian interglacial and Elsterian glacial. *Global and Planetary Change 227*, 104143. https://doi.org/10.1016/j.gloplacha.2023.104143.

Bayer, U., Scheck, M., Rabbel, W., Krawczyk, C. M., Götze, H. J., Stiller, M., Beilecke, T., Marotta, A.-M., Barrio-Alvers, L. & Kuder, J. 1999: An integrated study of the NE German Basin. *Tectonophysics 314*, 285–307. https://doi.org/10.1016/S0040-1951(99)00249-8.

Bense, V. F., Gleeson, T., Loveless, S. E., Bour, O. & Scibek, J. 2013: Fault zone hydrogeology. *Earth-Science Reviews 127*, 171–192. https://doi.org/10.1016/j.earscirev.2013.09.008.

BGR, LAGB, LBEG, LBGR, LLUR & LUNG 2022: Geologisches 3D-Modell tieferer Untergrund Norddeutsches Becken (TUNB). Available at: https://gst.bgr.de (accessed 03.06.2024).

Bijlsma, S. 1981: Fluvial sedimentation from the Fennoscandian area into the Northwest European Basin during the Late Cenozoic. *Geologie en Mijnbouw 8*, 337–345.

Bjarnadóttir, L. R., Winsborrow, M. C. M. & Andreassen, K. 2017: Large subglacial meltwater features in the central Barents Sea. *Geology 45*, 159–162. https://doi.org/10.1130/G38195.1.

Boulton, G. S., Hagdorn, M., Maillot, P. B. & Zatsepin, S. 2009: Drainage beneath ice sheets: groundwater–channel coupling, and the origin of esker systems from former ice sheets. *Quaternary Science Reviews 28*, 621–638. https://doi.org/10.1016/j.quascirev.2008.05.009.

Brandes, C., Plenefisch, T., Tanner, D. C., Gestermann, N. & Steffen, H. 2019: Evaluation of deep crustal earthquakes in northern Germany – possible tectonic causes. *Terra Nova 31*, 83–93. https://doi.org/10.1111/ter.12372.

Brandes, C., Polom, U., Winsemann, J. & Sandersen, P. B. E. 2022: The near-surface structure in the area of the Børglum fault, Sorgenfrei-Tornquist Zone, northern Denmark: implications for fault kinematics, timing of fault activity and fault control on tunnel valley formation. *Quaternary Science Reviews 289*, 107619. https://doi.org/10.1016/j.quascirev.2022.107619.

Brandes, C., Steffen, H., Steffen, R. & Wu, P. 2015: Intraplate seismicity in northern Central Europe is induced by the last glaciation. *Geology 43*, 611–614. https://doi.org/10.1130/G36710.1.

Breuer, S., Bebiolka, A., Noack, V. & Lang, J. 2023a: *Pleistozäne subglaziale Rinnen: Tiefe, Verbreitung und Bedeutung für die Mindesttiefe eines Endlagers.* 106 pp. Bundesanstalt für Geowissenschaften und Rohstoffe (BGR), Hannover. https://doi.org/10.25928/vrns-dg78.

Breuer, S., Bebiolka, A., Noack, V. & Lang, J. 2023b: The past is the key to the future – considering Pleistocene subglacial erosion for the minimum depth of a radioactive waste repository. *E&G Quaternary Science Journal 72*, 113–125. https://doi.org/10.5194/egqsj-72-113-2023.

Brose, F. 2005: Zur geomorphologischen Entwicklung Brandenburgs. *Brandenburgische Geowissenschaftliche Beiträge 12*, 153–163.

Brückner-Röhling, S., Espig, M., Fischer, M., Fleig, S., Forsbach, H., Kockel, F., Krull, P., Stiewe, H. & Wirth, H. 2002: *Standsicherheitsnachweise Nachbetriebsphase: Seismische Gefährdung – Teil 1: Strukturgeologie.* 183 pp. Bundesanstalt für Geowissenschaften und Rohstoffe (BGR), Hannover.

Brückner-Röhling, S., Fleig, S., Forsbach, H., Kockel, F., Krull, P. & Wirth, H. 2004: Die Bewegungsphasen tektonischer Störungen im Tertiär Norddeutschlands – Ergebnisse strukturgeologischer Untersuchungen. *Zeitschrift für Geologische Wissenschaften 5*, 295–301.

BurVal Working Group 2006: *Groundwater Resources in Buried Valleys: A Challenge for Geosciences.* 303 pp. Leibniz Institute for Applied Geosciences, Hannover.

Caine, J. S., Evans, J. P. & Forster, C. B. 1996: Fault zone architecture and permeability structure. *Geology 24*, 1025–1028. https://doi.org/10.1130/0091-7613(1996)024%3C1025:FZAAPS%3E2.3.CO;2.

Doornenbal, H., Abbink, O., Duin, E., Dusar, M., Hoth, P., Jasionowski, J., Lott, G., Mathiesen, A., Papiernik, B., Peryt, T., Veldkamp, H. & Wirth, H. 2010: Introduction, stratigraphic framework and mapping. *In* Doornenbal, H. & Stevenson, A. (eds.): *Petroleum Geological Atlas of the Southern Permian Basin Area*, 1–9. EAGE Publications, Houten.

Doornenbal, H. & Stevenson, A. 2010: *Petroleum Geological Atlas of the Southern Permian Basin Area*. 342 pp. EAGE Publications, Houten.

Ehlers, J. 1990: Reconstructing the dynamics of the north-west European Pleistocene ice sheets. *Quaternary Science Reviews 9*, 71–83. https://doi.org/10.1016/0277-3791(90)90005-U.

Ehlers, J. & Linke, G. 1989: The origin of deep buried channels of Elsterian age in Northwest Germany. *Journal of Quaternary Science 4*, 255–265. https://doi.org/10.1002/jqs.3390040306.

Ehlers, J., Grube, A., Stephan, H. J. & Wansa, S. 2011: Pleistocene glaciations of North Germany new results. *In* Ehlers, J., Gibbard, P. L. & Hughes, P. D. (eds.): *Quaternary Glaciations Extent and Chronology – A Closer Look*, 149–162. *Developments in Quaternary Science 15*. Elsevier, Amsterdam.

Ehlers, J., Meyer, K. D. & Stephan, H. J. 1984: The pre-Weichselian glaciations of north-west Europe. *Quaternary Science Reviews 3*, 1–40. https://doi.org/10.1016/0277-3791(84)90003-9.

Eissmann, L. 2002: Quaternary geology of eastern Germany (Saxony, Saxon-Anhalt, south Brandenburg, Thüringia), type area of the Elsterian and Saalian stages in Europe. *Quaternary Science Reviews 21*, 1275–1346. https://doi.org/10.1016/S0277-3791(01)00075-0.

Fischer, U. H., Bebiolka, A., Brandefelt, J., Cohen, D., Harper, J., Hirschorn, S., Jensen, M., Kennell, L., Liakka, J., Näslund, J. O., Normani, S., Stück, H. & Weitkamp, A. 2021: Radioactive waste under conditions of future ice ages. *In* Haeberli, W. & Whiteman, C. (eds.): *Snow and Ice-Related Hazards, Risks, and Disasters*, 323–375. Elsevier, Amsterdam. https://doi.org/10.1016/B978-0-12-817129-5.00005-6.

Gegg, L. & Preusser, F. 2023: Comparison of overdeepened structures in formerly glaciated areas of the northern Alpine foreland and northern central Europe. *E&G Quaternary Science Journal 72*, 23–36. https://doi.org/10.5194/egqsj-72-23-2023.

Hardt, J., Dooley, T. P. & Hudec, M. R. 2024: Physical modeling of ice-sheet-induced salt movements using the example of northern Germany. *Earth Surf Dynamics 12*, 559–579. https://doi.org/10.5194/esurf-12-559-2024.

Hardt, J., Norden, B., Bauer, K., Toelle, O. & Krambach, J. 2021: Surface cracks – geomorphological indicators for late quaternary halotectonic movements in Northern Germany. *Earth Surface Processes and Landforms 46*, 2963–2983. https://doi.org/10.1002/esp.5226.

Heidbach, O., Rajabi, M., Cui, X., Fuchs, K., Müller, B., Reinecker, J., Reiter, K., Tingay, M., Wenzel, F., Xie, F., Ziegler, M. O., Zoback, M. L. & Zoback, M. 2018: The world stress map database release 2016: crustal stress pattern across scales. *Tectonophysics 744*, 484–498. https://doi.org/10.1016/j.tecto.2018.07.007.

Hepp, D. A., Hebbeln, D., Kreiter, S., Keil, H., Bathmann, C., Ehlers, J. & Mörz, T. 2012: An east-west-trending Quaternary tunnel valley in the south-eastern North Sea and its seismic-sedimentological interpretation. *Journal of Quaternary Science 27*, 844–853. https://doi.org/10.1002/jqs.2599.

Hinsch, W. 1979: Rinnen an der Basis des glaziären Pleistozäns in Schleswig-Holstein. *Eiszeitalter und Gegenwart 29*, 173–178. https://doi.org/10.3285/eg.29.1.14.

Hönemann, G., Küstermann, W. & Meyer, W. 1995: Reflexionsseismische Kartierung von Tiefenlagen der Pleistozänbasis in Nordostdeutschland. *Zeitschrift für Geologische Wissenschaften 23*, 261–275.

Hughes, A. L. C., Gyllencreutz, R., Lohne, Ø. S., Mangerud, J. & Svendsen, J. I. 2016: The last Eurasian ice sheets – a chronological database and time-slice reconstruction, DATED-1. *Boreas 45*, 1–45. https://doi.org/10.1111/bor.12142.

Huster, H., Hübscher, C. & Seidel, E. 2020: Impact of Late Cretaceous to Neogene plate tectonics and Quaternary ice loads on supra-salt

15023085, 0, Downloaded from https://onlinelibrary.wiley.com/doi/10.1111/bor.12694 by Rwth Aachen University Universitatsbibliothek- 021000, Wiley Online Library on [27/01/2025]. See the Terms and Conditions (https://onlinelibrary.wiley.com/terms-and-conditions) on Wiley Online Library for rules of use; OA articles are governed by the applicable Creative Commons License

deposits at Eastern Glückstadt Graben, North German Basin. *International Journal of Earth Sciences 109*, 1029–1050. https://doi.org/10.1007/s00531-020-01850-8.

Huuse, M. & Lykke-Andersen, H. 2000: Overdeepened Quaternary valleys in the eastern Danish North Sea: morphology and origin. *Quaternary Science Reviews 19*, 1233–1253. https://doi.org/10.1016/S0277-3791(99)00103-1.

Huuse, M., Redfern, J., Le Heron, D. P., Dixon, R. J., Moscariello, A. & Craig, J. 2012: Glaciogenic reservoirs and hydrocarbon systems: an introduction. *In* Huuse, M., Redfern, J., Le Heron, D. P., Dixon, R. J., Moscariello, A. & Craig, J. (eds.): *Glaciogenic Reservoirs and Hydrocarbon Systems*, 1–28. Geological Society, London, Special Publications 368. https://doi.org/10.1144/SP368.19.

InSpEE 2015: Horizontal cross-section maps of Northern Germany. Available at: https://services.bgr.de/geologie/inspee_niveauschnitte (accessed 28.05.2024).

Jagemann, S. & Müller, C. O. 2023: Aktualisierung der Quartärbasis-tiefenkarte Sachsen-Anhalts. *Mitteilungen zu Geologie und Bergwesen von Sachsen-Anhalt 22*, 52–54.

Janszen, A., Moreau, J., Moscariello, A., Ehlers, J. & Kröger, J. 2013: Time-transgressive tunnel-valley infill revealed by a three-dimensional sedimentary model, Hamburg, north-west Germany. *Sedimentology 60*, 693–719. https://doi.org/10.1111/j.1365-3091.2012.01357.x.

Janszen, A., Spaak, M. & Moscariello, A. 2012: Effects of the substratum on the formation of glacial tunnel valleys: an example from the Middle Pleistocene of the southern North Sea Basin. *Boreas 41*, 629–643. https://doi.org/10.1111/j.1502-3885.2012.00260.x.

Jørgensen, F. & Sandersen, P. B. 2006: Buried and open tunnel valleys in Denmark – erosion beneath multiple ice sheets. *Quaternary Science Reviews 25*, 1339–1363. https://doi.org/10.1016/j.quascirev.2005.11.006.

Kaiser, A., Reicherter, K., Hübscher, C. & Gajewski, D. 2005: Variation of the present-day stress field within the North German Basin – insights from thin shell FE modeling based on residual GPS velocities. *Tectonophysics 397*, 55–72. https://doi.org/10.1016/j.tecto.2004.10.009.

Kehew, A., Piotrowski, J. & Jørgensen, F. 2012: Tunnel valleys: concepts and controversies – a review. *Earth-Science Reviews 113*, 33–58. https://doi.org/10.1016/j.earscirev.2012.02.002.

Kirkham, J. D., Hogan, K. A., Larter, R. D., Arnold, N. S., Ely, J. C., Clark, C. D., Self, E., Games, K., Huuse, M., Stewart, M. A., Ottesen, D. & Dowdeswell, J. A. 2024a: Tunnel valley formation beneath deglaciating mid-latitude ice sheets: observations and modelling. *Quaternary Science Reviews 323*, 107680.

Kirkham, J. D., Hogan, K. A., Larter, R. D., Self, E., Games, K., Huuse, M., Stewart, M. A., Ottesen, D., Arnold, N. S. & Dowdeswell, J. A. 2021: Tunnel valley infill and genesis revealed by high-resolution 3-D seismic data. *Geology 49*, 1516–1520. https://doi.org/10.1130/G49048.1.

Kirkham, J. D., Hogan, K. A., Larter, R. D., Self, E., Games, K., Huuse, M., Stewart, M. A., Ottesen, D., Le Heron, D. P., Lawrence, A., Kane, I., Arnold, N. S. & Dowdeswell, J. A. 2024b: The infill of tunnel valleys in the central North Sea: implications for sedimentary processes, geohazards and ice-sheet dynamics. *Marine Geology 467*, 107185. https://doi.org/10.1016/j.margeo.2023.107185.

Kley, J. & Voigt, T. 2008: Late Cretaceous intraplate thrusting in central Europe: Effect of Africa-Iberia-Europe convergence, not Alpine collision. *Geology 36*, 839–842. https://doi.org/10.1130/G24930A.1.

Knox, R., Bosch, A., Skovbjerg Rasmussen, E., Heilmann-Clausen, C., Hiss, M., de Lugt, I., Kasínski, J., King, C., Köthe, A., Słodowska, B., Standke, G. & Vandenberghe, N. 2010: Cenozoic. *In* Doornenbal, H. & Stevenson, A. (eds.): *Petroleum Geological Atlas of the Southern Permian Basin Area*, 211–223. EAGE, Houten.

Kristensen, T. B. & Huuse, M. 2012: Multistage erosion and infill of buried Pleistocene tunnel valleys and associated seismic velocity effects. *In* Huuse, M., Redfern, J., Le Heron, D. P., Dixon, R. J., Moscariello, A. & Craig, J. (eds.): *Glaciogenic Reservoirs and Hydrocarbon Systems*, 159–172. Geological Society, London, Special Publication 368. https://doi.org/10.1144/SP368.15.

Kristensen, T. B., Piotrowski, J. A., Huuse, M., Clausen, O. R. & Hamberg, L. 2008: Time-transgressive tunnel valley formation indicated by infill sediment structure, North Sea – the role of glaciohydraulic supercooling. *Earth Surface Processes and Landforms 33*, 546–559. https://doi.org/10.1002/esp.1668.

Kuster, H. & Meyer, K. D. 1979: Glaziäre Rinnen im mittleren und nördlichen Niedersachsen. *Eiszeitalter und Gegenwart 29*, 135–156. https://doi.org/10.3285/eg.29.1.12.

Lang, J. & Hampel, A. 2023: Deformation of salt structures by ice-sheet loading: insights into the controlling parameters from numerical modelling. *International Journal of Earth Sciences 112*, 1133–1155. https://doi.org/10.1007/s00531-023-02295-5.

Lang, J., Böhner, U., Polom, U., Serangeli, J. & Winsemann, J. 2015: The Middle Pleistocene tunnel valley at Schöningen as a Paleolithic archive. *Journal Human of Evolution 89*, 18–26. https://doi.org/10.1016/j.jhevol.2015.02.004.

Lang, J., Hampel, A., Brandes, C. & Winsemann, J. 2014: Response of salt structures to ice-sheet loading: implications for ice-marginal and subglacial processes. *Quaternary Science Reviews 101*, 217–233. https://doi.org/10.1016/j.quascirev.2014.07.022.

Lang, J., Lauer, T. & Winsemann, J. 2018: New age constraints for the Saalian glaciation in northern central Europe: implications for the extent of ice sheets and related proglacial lake systems. *Quaternary Science Reviews 180*, 240–259. https://doi.org/10.1016/j.quascirev.2017.11.029.

Lang, J., Winsemann, J., Steinmetz, D., Polom, U., Pollok, L., Böhner, U., Serangeli, J., Brandes, C., Hampel, A. & Winghart, S. 2012: The Pleistocene of Schöningen, Germany: a complex tunnel valley fill revealed from 3D subsurface modelling and shear wave seismics. *Quaternary Science Reviews 39*, 86–105. https://doi.org/10.1016/j.quascirev.2012.02.009.

Lauer, T. & Weiss, M. 2018: Timing of the Saalian-and Elsterian glacial cycles and the implications for Middle Pleistocene hominin presence in central Europe. *Scientific Reports 8*, 5111. https://doi.org/10.1038/s41598-018-23541-w.

Litt, T., Behre, K. E., Meyer, K. D., Stephan, H. J. & Wansa, S. 2007: Stratigraphische Begriffe für das Quartär des norddeutschen Vereisungsgebietes. *E&G Quaternary Science Journal 56*, 7–65. https://doi.org/10.23689/fidgeo-1278.

Lohr, T., Krawczyk, C. M., Tanner, D. C., Samiee, R., Endres, H., Oncken, O., Trappe, H. & Kukla, P. A. 2007: Strain partitioning due to salt: insights from interpretation of a 3D seismic data set in the NW German Basin. *Basin Research 19*, 579–597. https://doi.org/10.1111/j.1365-2117.2007.00338.x.

Lohrberg, A., Krastel, S., Unverricht, D. & Schwarzer, K. 2022a: The Heligoland Glacitectonic Complex in the southeastern North Sea: indicators of a pre- or early-Elsterian ice margin. *Boreas 51*, 100–117. https://doi.org/10.1111/bor.12551.

Lohrberg, A., Schneider von Deimling, J., Grob, H., Lenz, K. F. & Krastel, S. 2022b: Tunnel valleys in the southeastern North Sea: more data, more complexity. *E&G Quaternary Science Journal 71*, 267–274. https://doi.org/10.5194/egqsj-71-267-2022.

Lohrberg, A., Schwarzer, K., Unverricht, D., Omlin, A. & Krastel, S. 2020: Architecture of tunnel valleys in the southeastern North Sea: new insights from high-resolution seismic imaging. *Journal of Quaternary Science 35*, 892–906. https://doi.org/10.1002/jqs.3244.

Ludwig, A. O. 2001: Vertical movements since the beginning of the Rupelian stage. *Brandenburgische Geowissenschaftliche Beiträge 8*, 5–12.

Ludwig, A. O. & Stackebrandt, W. 2010: Neotektonisches Bewegungsverhalten. *In* Stackebrandt, W. & Manhenke, V. (eds.): *Atlas zur Geologie von Brandenburg*, 68–69. Landesamt für Bergbau, Geologie und Rohstoffe Brandenburg (LBGR), Cottbus.

LUNG MV 2023: Kartenportal Umwelt Mecklenburg. Available at: https://www.umweltkarten.mv-regierung.de/atlas/script/index.php (accessed 01.12.2023).

Lüthgens, C., Böse, M. & Krbetschek, M. 2010: On the age of the young morainic morphology in the area ascribed to the maximum extent of the Weichselian glaciation in north-eastern Germany. *Quaternary International 222*, 72–79. https://doi.org/10.1016/j.quaint.2009.06.028.

Lüthgens, C., Hardt, J. & Böse, M. 2020: Proposing a new conceptual model for the reconstruction of ice dynamics in the SW sector of the Scandinavian Ice Sheet (SIS) based on the reinterpretation of

15023085, 0, Downloaded from https://onlinelibrary.wiley.com/doi/10.1111/bor.12694 by Rwth Aachen University Universitatsbibliothek- 021000, Wiley Online Library on [27/01/2025]. See the Terms and Conditions (https://onlinelibrary.wiley.com/terms-and-conditions) on Wiley Online Library for rules of use; OA articles are governed by the applicable Creative Commons License

published data and new evidence from optically stimulated luminescence (OSL) dating. *E&G Quaternary Science Journal 69*, 201–223. https://doi.org/10.5194/egqsj-69-201-2020.
Lutz, R., Kalka, S., Gaedicke, C., Reinhardt, L. & Winsemann, J. 2009: Pleistocene tunnel valleys in the German North Sea: spatial distribution and morphology. *Zeitschrift der Deutschen Gesellschaft für Geowissenschaften 160*, 225–235. https://doi.org/10.1127/1860-1804/2009/0160-0225.
Marotta, A. M., Bayer, U., Thybo, H. & Scheck, M. 2002: Origin of the regional stress in the North German basin: results from numerical modelling. *Tectonophysics 360*, 245–264. https://doi.org/10.1016/S0040-1951(02)00358-X.
Maystrenko, Y., Bayer, U., Brink, H. J. & Littke, R. 2008: The Central European basin system – an overview. *In* Littke, R., Bayer, U., Gajewski, D. & Nelskamp, S. (eds.): *Dynamics of Complex Intracontinental Basins – The Central European Basin System*, 16–34. Springer, Berlin.
Maystrenko, Y., Bayer, U. & Scheck-Wenderoth, M. 2005: The Glueckstadt Graben, a sedimentary record between the North and Baltic Sea in north Central Europe. *Tectonophysics 397*, 113–126. https://doi.org/10.1016/j.tecto.2004.10.004.
Maystrenko, Y. P., Bayer, U. & Scheck-Wenderoth, M. 2013: Salt as a 3D element in structural modeling – example from the Central European Basin System. *Tectonophysics 591*, 62–82. https://doi.org/10.1016/j.tecto.2012.06.030.
Molnar, P., Anderson, R. S. & Anderson, S. P. 2007: Tectonics, fracturing of rock, and erosion. *Journal of Geophysical Research: Earth Surface 112*, F03014. https://doi.org/10.1029/2005JF000433.
Morawietz, S., Heidbach, O., Reiter, K., Ziegler, M., Rajabi, M., Zimmermann, G., Müller, B. & Tingay, M. 2020: An open-access stress magnitude database for Germany and adjacent regions. *Geothermal Energy 8*, 25. https://doi.org/10.1186/s40517-020-00178-5.
Müller, C., Jähne-Klingberg, F., von Goerne, G., Binot, F. & Röhling, H. G. 2016: Vom Geotektonischen Atlas ("Kockel-Atlas") zu einem 3D-Gesamtmodell des Norddeutschen Beckens: Basisinformationen zum tieferen Untergrund von Norddeutschland. *Zeitschrift der Deutschen Gesellschaft für Geowissenschaften 167*, 65–106. https://doi.org/10.1127/zdgg/2016/0072.
Müller, K., Winsemann, J., Tanner, D. C., Lege, T., Spies, T. & Brandes, C. 2022: Glacially induced faults in Germany. *In* Steffen, H., Olesen, O. & Sutinen, R. (eds.): *Glacially-Triggered Faulting*, 283–303. Cambridge University Press, Cambridge.
Ó Cofaigh, C. 1996: Tunnel valley genesis. *Progress in Physical Geography 20*, 1–19. https://doi.org/10.1177/030913339602000101.
Ottesen, D., Stewart, M., Brönner, M. & Batchelor, C. L. 2020: Tunnel valleys of the central and northern North Sea (56°N to 62°N): distribution and characteristics. *Marine Geology 425*, 106199. https://doi.org/10.1016/j.margeo.2020.106199.
Passchier, S., Laban, C., Mesdag, C. S. & Rijsdijk, K. F. 2010: Subglacial bed conditions during Late Pleistocene glaciations and their impact on ice dynamics in the southern North Sea. *Boreas 39*, 633–647. https://doi.org/10.1111/j.1502-3885.2009.00138.x.
Patton, H., Hubbard, A., Andreassen, K., Winsborrow, M. & Stroeven, A. P. 2016: The build-up, configuration, and dynamical sensitivity of the Eurasian ice-sheet complex to Late Weichselian climatic and oceanic forcing. *Quaternary Science Reviews 153*, 97–121. https://doi.org/10.1016/j.quascirev.2016.10.009.
Pharaoh, T. C., Dusar, M., Geluk, M., Kockel, F., Krawczyk, C. M., Krzywiec, P., Scheck-Wenderoth, M., Thybo, H., Vejbæk, O. V. & Van Wees, J. D. 2010: Tectonic evolution. *In* Doornenbal, H. & Stevenson, A. (eds.): *Petroleum Geological Atlas of the Southern Permian Basin Area*, 25–57. EAGE, Houten.
Piña-Valdés, J., Socquet, A., Beauval, C., Doin, M. P., D'Agostino, N. & Shen, Z. K. 2022: 3D GNSS velocity field sheds light on the deformation mechanisms in Europe: effects of the vertical crustal motion on the distribution of seismicity. *Journal of Geophysical Research: Solid Earth 127*, e2021JB023451. https://doi.org/10.1029/2021JB023451.
Piotrowski, J. A. 1994: Tunnel-valley formation in northwest Germany – geology, mechanisms of formation and subglacial bed conditions for the Bornhöved tunnel valley. *Sedimentary Geology 89*, 107–141. https://doi.org/10.1016/0037-0738(94)90086-8.
Piotrowski, J. A. 1997: Subglacial hydrology in north-western Germany during the last glaciation: groundwater flow, tunnel valleys and hydrological cycles. *Quaternary Science Reviews 16*, 169–185. https://doi.org/10.1016/S0277-3791(96)00046-7.
Piotrowski, J. A., Geletneky, J. & Vater, R. 1999: Soft-bedded subglacial meltwater channel from Welzow-Süd open-cast lignite mine, Lower Lusatia, eastern Germany. *Boreas 28*, 363–374. https://doi.org/10.1111/j.1502-3885.1999.tb00226.x.
Ravier, E., Buoncristiani, J. F., Guiraud, M., Menzies, J., Clerc, S., Goupy, B. & Portier, E. 2014: Porewater pressure control on subglacial soft sediment remobilization and tunnel valley formation: a case study from the Alnif tunnel valley (Morocco). *Sedimentary Geology 304*, 71–95. https://doi.org/10.1016/j.sedgeo.2014.02.005.
Ravier, E., Buoncristiani, J. F., Menzies, J., Guiraud, M., Clerc, S. & Portier, E. 2015: Does porewater or meltwater control tunnel valley genesis? Case studies from the Hirnantian of Morocco. *Palaeogeography, Palaeoclimatology Palaeoecology 418*, 359–376. https://doi.org/10.1016/j.palaeo.2014.12.003.
Reicherter, K., Kaiser, A. & Stackebrandt, W. 2005: The post-glacial landscape evolution of the North German Basin: morphology, neotectonics and crustal deformation. *International Journal of Earth Sciences 94*, 1083–1093. https://doi.org/10.1007/s00531-005-0007-0.
Reinhold, K., Krull, P. & Kockel, F. 2008: *Salzstrukturen Norddeutschlands, 1:500.000*. Bundesanstalt für Geowissenschaften und Rohstoffe, Hannover.
Röckel, L., Ahlers, S., Müller, B., Reiter, K., Heidbach, O., Henk, A., Hergert, T. & Schilling, F. 2022: The analysis of slip tendency of major tectonic faults in Germany. *Solid Earth 13*, 1087–1105. https://doi.org/10.5194/se-13-1087-2022.
Roskosch, J., Winsemann, J., Polom, U., Brandes, C., Tsukamoto, S., Weitkamp, A., Bartholomäus, W. A., Henningsen, D. & Frechen, M. 2015: Luminescence dating of ice-marginal deposits in northern Germany: evidence for repeated glaciations during the Middle Pleistocene (MIS 12 to MIS 6). *Boreas 44*, 103–126. https://doi.org/10.1111/bor.12083.
Sandersen, P. B. E. & Jørgensen, F. 2012: Substratum control on tunnel-valley formation in Denmark. *In* Huuse, M., Redfern, J., Le Heron, D. P., Dixon, R. J., Moscariello, A. & Craig, J. (eds.): *Glaciogenic Reservoirs and Hydrocarbon Systems*, 145–157. Geological Society, London, Special Publications 368. https://doi.org/10.1144/SP368.12.
Sandersen, P. B. E. & Jørgensen, F. 2022: Tectonic impact on Pleistocene and Holocene erosional patterns in a formerly glaciated intra-plate area. *Quaternary Science Reviews 293*, 107681. https://doi.org/10.1016/j.quascirev.2022.107681.
Scheck, M., Bayer, U., Otto, V., Lamarche, J., Banka, D. & Pharaoh, T. 2002: The Elbe Fault System in North Central Europe – a basement controlled zone of crustal weakness. *Tectonophysics 360*, 281–299. https://doi.org/10.1016/S0040-1951(02)00357-8.
Scheck-Wenderoth, M. & Lamarche, J. 2005: Crustal memory and basin evolution in the Central European Basin System – new insights from a 3D structural model. *Tectonophysics 397*, 143–165. https://doi.org/10.1016/j.tecto.2004.10.007.
Schulz, R. 2002: Forschungsbohrungen des GGA-Instituts. *Zeitschrift für Angewandte Geologie 48*, 3–8.
Schütze, J. 2024: Qualitative Korrelation von subglazialen Rinnen mit geologischen Strukturen im Untergrund. B.Sc. thesis, RWTH Aachen, 48 pp.
Schwarz, C. 1996: Neue Befunde zur Verbreitung und Dimension pleistozäner Rinnensysteme auf dem deutschen Nordseeschelf. *Geologisches Jahrbuch A 146*, 233–244.
Shreve, R. L. 1972: Movement of water in glaciers. *Journal of Glaciology 11*, 205–214. https://doi.org/10.3189/S002214300002219X.
Smed, P. 1998: Die Entstehung der dänischen und norddeutschen Rinnentäler (Tunneltäler) – Glaziologische Gesichtspunkte. *Eiszeitalter und Gegenwart 48*, 1–18. https://doi.org/10.3285/eg.48.1.01.
Stackebrandt, W. 2004: Zur Neotektonik in Norddeutschland. *Zeitschrift für Geologische Wissenschaften 32*, 85–95.
Stackebrandt, W. 2009: Subglacial channels of northern Germany – a brief review. *ZDGG 160*, 203–210. https://doi.org/10.1127/1860-1804/2009/0160-0203.
Stewart, M. A. & Lonergan, L. 2011: Seven glacial cycles in the middle-late Pleistocene of northwest Europe: geomorphic evidence from

15023885, 0, Downloaded from https://onlinelibrary.wiley.com/doi/10.1111/bor.12694 by Rwth Aachen University Universitatsbibliothek- 021000, Wiley Online Library on [27/01/2025]. See the Terms and Conditions (https://onlinelibrary.wiley.com/terms-and-conditions) on Wiley Online Library for rules of use; OA articles are governed by the applicable Creative Commons License

buried tunnel valleys. *Geology 39*, 283–286. https://doi.org/10.1130/G31631.1.

Stewart, M. A., Lonergan, L. & Hampson, G. 2013: 3D seismic analysis of buried tunnel valleys in the central North Sea: morphology, cross-cutting generations and glacial history. *Quaternary Science Reviews 72*, 1–17. https://doi.org/10.1016/j.quascirev.2013.03.016.

Talbot, C. J. 1999: Ice ages and nuclear waste isolation. *Engineering Geology 52*, 177–192. https://doi.org/10.1016/S0013-7952(99)00005-8.

Thöle, H., Gaedicke, C., Kuhlmann, G. & Reinhardt, L. 2014: Late Cenozoic sedimentary evolution of the German North Sea – A seismic stratigraphic approach. *Newsletters on Stratigraphy 47*, 299–329. https://doi.org/10.1127/0078-0421/2014/0049.

Toucanne, S., Zaragosi, S., Bourillet, J. F., Gibbard, P. L., Eynaud, F., Giraudeau, J., Turon, J. L., Cremer, M., Cortijo, E., Martinez, P. & Rossignol, L. 2009: A 1.2 Ma record of glaciation and fluvial discharge from the West European Atlantic margin. *Quaternary Science Reviews 28*, 2974–2981. https://doi.org/10.1016/j.quascirev.2009.08.003.

Tylmann, K., Rinterknecht, V. R., Woźniak, P. P., Guillou, V. & ASTER Team 2022: Asynchronous dynamics of the last Scandinavian Ice Sheet along the Pomeranian ice-marginal belt: a new scenario inferred from surface exposure 10Be dating. *Quaternary Science Reviews 294*, 107755. https://doi.org/10.1016/j.quascirev.2022.107755.

Urai, J. L., Schléder, Z., Spiers, C. J. & Kukla, P. A. 2008: Flow and transport properties of salt rocks. *In* Littke, R., Bayer, U., Gajewski, D. & Nelskamp, S. (eds.): *Dynamics of Complex Intracontinental Basins – The Central European Basin System*, 277–290. Springer, Berlin.

Van der Vegt, P., Janszen, A. & Moscariello, A. 2012: Tunnel valleys: current knowledge and future perspectives. *In* Huuse, M., Redfern, J., Le Heron, D. P., Dixon, R. J., Moscariello, A. & Craig, J. (eds.): *Glaciogenic Reservoirs and Hydrocarbon Systems*, 75–97. Geological Society, London, Special Publications 368. https://doi.org/10.1144/sp368.13.

Van Gessel, S. and 53 others. 2021: The HIKE European Fault Database (EFDB) compiled in the framework of the GeoERA project HIKE (2018–2021). Available at: https://egdi.geology.cz/record/basic/5edf7bd4-9270-4188-b69d-7ddd0a010833 (accessed 10.11.2023).

Voigt, T., Kley, J. & Voigt, S. 2021: Dawn and dusk of Late Cretaceous basin inversion in central Europe. *Solid Earth 12*, 1443–1471. https://doi.org/10.5194/se-12-1443-2021.

Warsitzka, M., Jähne-Klingberg, F., Kley, J. & Kukowski, N. 2019: The timing of salt structure growth in the Southern Permian Basin (Central Europe) and implications for basin dynamics. *31*, 337–360. https://doi.org/10.1111/bre.12323.

Wenau, S. & Alves, T. M. 2020: Salt-induced crestal faults control the formation of Quaternary tunnel valleys in the southern North Sea. *Boreas 49*, 799–812. https://doi.org/10.1111/bor.12461.

Winsemann, J., Brandes, C., Polom, U. & Weber, C. 2011: Depositional architecture and palaeogeographic significance of Middle Pleistocene glaciolacustrine ice marginal deposits in northwestern Germany: a synoptic overview. *E&G Quaternary Science Journal 60*, 212–235. https://doi.org/10.3285/eg.60.2-3.01.

Winsemann, J., Koopmann, H., Tanner, D. C., Lutz, R., Lang, J., Brandes, C. & Gaedicke, C. 2020: Seismic interpretation and structural restoration of the Heligoland glaciotectonic thrust-fault complex: implications for multiple deformation during (pre-) Elsterian to Warthian ice advances into the southern North Sea Basin. *Quaternary Science Reviews 227*, 106068. https://doi.org/10.1016/j.quascirev.2019.106068.

Ziegler, P. A. 1990: Collision related intra-plate compression deformations in western and central Europe. *Journal of Geodynamics 11*, 357–388. https://doi.org/10.1016/0264-3707(90)90017-O.

Ziegler, P. A. 1992: European Cenozoic rift system. *Tectonophysics 208*, 91–111. https://doi.org/10.1016/0040-1951(92)90338-7.

15023885, 0, Downloaded from https://onlinelibrary.wiley.com/doi/10.1111/bor.12694 by Rwth Aachen University Universitatsbibliothek- 021000, Wiley Online Library on [27/01/2025]. See the Terms and Conditions (https://onlinelibrary.wiley.com/terms-and-conditions) on Wiley Online Library for rules of use; OA articles are governed by the applicable Creative Commons License